ISTANBUL TECHNICAL UNIVERSITY ★ INSTITUTE OF SCIENCE AND TECHNOLOGY

SYNTHESIS AND CHARACTERIZATION OF ELECTRICALLY CONDUCTIVE POLYPYRROLE DERIVATIVES-POLY(ACRYLONITRILE-CO-METHYL METHACRYLATE) COMPOSITES AND NANOFIBER FORMATION

M.Sc. THESIS

Ulviye DALGIÇ

Department of Polymer Science and Technology

Polymer Science and Technology Programme

MARCH 2012

ISTANBUL TECHNICAL UNIVERSITY ★ INSTITUTE OF SCIENCE AND TECHNOLOGY

SYNTHESIS AND CHARACTERIZATION OF ELECTRICALLY CONDUCTIVE POLYPYRROLE DERIVATIVES-POLY(ACRYLONITRILE-CO-METHYL METHACRYLATE) COMPOSITES AND NANOFIBER FORMATION

M.Sc. THESIS

Ulviye DALGIÇ
(515071035)

Department of Polymer Science and Technology

Polymer Science and Technology Programme

Thesis Advisor: Prof. Dr. A. Sezai SARAÇ

MARCH 2012

İSTANBUL TEKNİK ÜNİVERSİTESİ ★ FEN BİLİMLERİ ENSTİTÜSÜ

İLETKEN POLİPİROL TÜREVLERİ-POLİ(AKRİLONİTRİL-KO-METİL METAKRİLAT) KOMPOZİT İNCE FİLM VE NANOLİF OLUŞUMU VE KARAKTERİZASYONU

YÜKSEK LİSANS TEZİ

Ulviye DALGIÇ
(515071035)

Polimer Bilim ve Teknolojisi Anabilim Dalı

Polimer Bilim ve Teknolojisi Programı

Tez Danışmanı: Prof. Dr. A. Sezai SARAÇ

Mart 2012

Ulviye Dalgıç, a **M.Sc.** student of ITU **Institute of Science and Technology** student ID **515071035**, successfully defended the **thesis** entitled "**SYNTHESIS AND CHARACTERIZATION OF ELECTRICALLY CONDUCTIVE POLYPYRROLE DERIVATIVES-POLY(ACRYLONITRILE-CO-METHYL METHACRYLATE) COMPOSITES AND NANOFIBER FORMATION**", which she prepared after fulfilling the requirements specified in the associated legislations, before the jury whose signatures are below.

Thesis Advisor :	**Prof. Dr. A. Sezai SARAÇ** İstanbul Technical University	.....
Jury Members :	**Prof. Dr. Ahmet AKAR** İstanbul Technical University	.....
	Assoc. Prof. Dr. Hale KARAKAŞ İstanbul Technical University	.....

Date of Submission : 30 January 2012
Date of Defense : 20 March 2012

To my family,

FOREWORD

I would like to express my deep appreciation and thanks for my advisor Prof. Dr. A. Sezai SARAÇ. I am grateful to my family for their everlasting support.

I am also thankful to my collegues Nazif Uğur KAYA, Timuçin BALKAN, Suat ÇETİNER, Bilge KILIÇ, Cansev TEZCAN, Cem ÜNSAL, Damla ECEVİT, Fatma Gül GÜLER, S.Esra ÖZGÜL, Aslı GENÇTÜRK for their helps and composing our warm office atmosphere.

This work is supported by ITU Institute of Science and Technology.

January 2012

Ulviye DALGIÇ
Chemical Engineer

TABLE OF CONTENTS

Page

ABBREVIATIONS

MMA	:Methyl Methacrylate
PMMA	:Polymetyl methacrylate
AN	:Acrylonitrile
PAN	:Polyacrylonitrile
Py	:Pyrrole
PPy	:Polypyrrole
NPhPy	:N-Phenyl Pyrrole
PNPhPy	:Poly(N-Phenyl Pyrrole)
NMPy	:N-Methyl Pyrrole
PNMPy	:Poly(N-Methyl Pyrrole)
KPS	:Potassium Persulfate
CAN	:Ceric Ammonium Nitrate
DBSA	:Dodecylbenzensulfonic Acid Sodium Salt
DMF	:Dimethylformamide
DSC	:Differential Scanning Calorimetry
FT-IR	:Fourrier Transform Infrared
NMR	:Nuclear Magnetic Resonance
SEM	:Scanning Electron Microscope
T_g	:Glass Transition Temperature
P(MMA-co-AN)	:Poly(methyl methacrylate-co-acrylonitrile)
PPy/P(MMA-co-AN)	:Polypyrrole/Poly(methylmethacrylate-co-acrylonitrile)
PNMPy/P(MMA-co-AN)	:Poly(N-Methyl Pyrrole)/Poly(methyl methacrylate-co-acrylonitrile)
PNPhPy/P(MMA-co-AN)	:Poly(N-Phenyl Pyrrole)/Poly(methyl methacrylate-co-acrylonitrile)

LIST OF TABLES

Page

LIST OF FIGURES

Page

SYNTHESIS AND CHARACTERIZATION OF ELECTRICALLY CONDUCTIVE POLYPYRROLE DERIVATIVES-POLY(ACRYLONITRILE-CO-METHYL METHACRYLATE) COMPOSITES AND NANOFIBER FORMATION

SUMMARY

This study can be categorized into two parts. The first part aims to synthesis new polymeric nanocomposite materials which can be used for electromagnetic interference shielding and absorbent panel applications. In-situ polymerized polypyrrole (PPy), poly(N-Methyl Pyrrole) (PNMPy) and poly(N-phenylpyrrole) (PNPhPy) on P(MMA-co-AN) matrix were used as composite thin films. First, emulsion polymerization of acrylonitrile (AN) and methyl methacrylate (MMA) initiated by potassium persulfate (KPS) in the aqueous medium was performed. Afterwards, pyrrole (Py), N-Methyl Pyrrole (PNMPy) and N-phenyl pyrrole (NPhPy) were polymerized on P(MMA-co-AN) matrix in dimethylformamide (DMF). Ce(IV) salt was used as an oxidant polymerization of Py, NMPy and NPhPy on P(MMA-co-AN) matrix. Composite films were then acquired by evaporation of DMF. By the increase in the amount of pyrrole derivatives in the composite film, AC conductivity, dielectric constants and dielectric loss increased. In all samples, real permittivity (Eps') and imaginary permittivity (Eps") decreased as the frequency (f) increased; they remained stable in the region of 10 Hz to 10^7. -H atoms related to PPy did not enhance conductivity and dielectric permittivity values of composite films as compared to PNPhPy including of those due to less polarization of –H atoms than phenyl groups. Spectroscopic, morphologic and thermal chracterization of composite films were performed by FTIR-ATR, UV-Visible spectrometer, Nuclear Magnetic Resonance (NMR), scanning electron microscopy (SEM), Differential Scanning Calorimeter (DSC).

In the second part, PPy derivatives-P(MMA-co-AN) based nanofibers for use new generation products such as electrostatic discharge, sensors application in textile industry were obtained. The oxidative polymerization of pyrrole (Py) derivatives by cerium (IV) on the poly(methyl methacrylate-co-acrylonitrile) copolymer matrix was performed. Nanofibers were obtained from this solution by electrospinning method.The properties of nanofibers were evaluated by FTIR-ATR spectroscopy, UV-Visible spectrometer and scanning electron microscopy. A new absorption band was observed corresponding the CH in plane vibration of polypyrrole by FTIR-ATR analysis. A linear relationship was determined between the absorbance ratios of functional groups corresponding to the conjugated polymeric units and initial Py derivatives concentration. Scanning electron microscope images indicated that the diameters of nanofibers were dependent on PPy derivatives content and that the average nanofiber diameters were reduced by increasing the initially added Py derivatives content.

İLETKEN POLİPİROL TÜREVLERİ-POLİ(AKRİLONİTRİL-KO-METİL METAKRİLAT) KOMPOZİT İNCE FİLM VE NANOLİF OLUŞUMU VE KARAKTERİZASYONU

ÖZET

Bu çalışma iki bölümden oluşmaktadır. Birinci bölümde, elektromanyetik kalkan ve absorban panel uygulamalarında kullanılmak üzere yeni, polimerik nanokompozit malzemeler sentezlemek amaçlanmıştır. P(MMA-ko-AN) kopolimeri üzerinde polimerleşen polipirol (PPy), poli n-metilpirol (PNMPy), poli n-fenilpirol (PNPhPy) ince kompozit film olarak kullanılmıştır. İlk önce, metil metakrilat ve akrilonitrilin emulsiyon polimerizasyonu, potasyum persulfat başlatıcısı kullanılarak su ortamında yapılmıştır. Daha sonra, Py, MPy ve NFPy' nin dimetilformamid (DMF) içerisinde çözülmüş P(MMA-ko-AN) matrisinde polimerizasyonları gerçekleştirilmiştir. Ce(IV) tuzu, Py, NMPy ve NFPy' nin polimerleştirilmesinde oksidant olarak kullanılmıştır. Oluşturulan kompozitlerin filmleri çözücünün (DMF) uzaklaştırılmasıyla elde edilmiştir. Kompozit film içerisindeki pirol miktarının artması ile AC iletkenlik, dielektrik sabitleri ve dielektrik kaybı artmıştır. Bütün film örneklerinde, dielektrik sabiti (Eps') ve dielektrik kaybı (Eps") artan frekans (f) ile birlikte azalma göstermiş; 10 Hz ile 10^7 Hz aralığında sabit bir değer göstermiştir. PPy' ye ait –H atomlarının iletkenlik ve dielektrik geçirgenlik değerlerine katkıları, PNFPy' ye ait fenil gruplarınınkinden daha az olmuştur. Bunun sebebi yan grup olan fenil gruplarının, -H atomlarına oranla iletken polimer zincirine daha polar bir yapı kazandırmasıdır. Kompozit filmlerin spektroskopik, morfolojik ve termal karakterizasyonu FTIR-ATR, UV-Görünür bölge spektrometresi, çekirdek manyetik rezonansı (NMR), taramalı elektron mikroskobu (SEM), diferansiyel taramalı kalorimetri (DSC).

Çalışmanın ikinci bölümünde, tekstil endüstrisinde yeni nesil ürünlerde elektrostatik deşarj, sensor gibi uygulama alanlarında kullanılmak üzere polipirol türevleri/poli(metil metakrilat-ko-akrilonitril) bazlı nano liflerin eldesi amaçlanmıştır. Pirol türevlerinin poli(metil metakrilat-ko-akrilonitril) kopolimer matrisinde oksidatif polimerizasyonu gerçekleştirilmiş ve bu çözeltiden elektrospin metodu ile nano lifler elde edilmiştir. Nano liflerin özellikleri FTIR-ATR spektroskopisi, UV-Görünür bölge spektrometresi ve taramalı elektron mikroskobu (SEM) yardımıyla değerlendirilmiştir. FTIR-ATR analizi sonucu polipirol türevleri oluşumundan sonra polipirol türevlerine ait CH pikinin titreşimi elde edilmiştir. Bu gruba ait pikin polipirol türevleri oluşumuna bağlı olarak, başlangıçta eklenen pirol türevi miktarı ile lineer bir ilişki olduğu belirlenmiştir. Taramalı elektron mikroskop görüntüleri nano liflerin çaplarının polipirol türevi miktarına bağlı olduğunu ve ortalama nano lif çaplarının başlangıçta eklenen pirol türevi miktarının artması ile azaldığını göstermiştir.

Bu çalışma, elekriksel iletken yapılarının antistatik, elektrostatik boşalma ve elektromanyetik koruma uygulamaları için yeni fonksiyonel polimerik nanokompozitlerin sentezini kapsar. Elektromanyetik koruma, elektromanyetik dalgaların boşluğa yönelimini, iletken malzemelerden yapılmış bir bariyer ile bloke ederek korumaktadır. Bu tez çalışmasında, P(MMA-co-AN) kopolimerinin üstün mekanik özellikleri, polipirol ve türevlerinin iletkenlik özelliği ile birleştirilerek, zararlı elektromanyetik dalgalara karşı koruyucu olma potansiyeline sahip iletken PPy türevleri-P(MMA-co-AN) kompozit yapılar hazırlanmıştır.

Poli(metil metakrilat-ko-akrilonitril) (P(MMA-ko-AN)) kopolimeri bir termometre, mekanik bir karıştırıcı ve bir geri akış kondansatörü ile donatılmış bir cam reaktör içinde, 70^{o}C'de, su ortamında emulsiyon polimerizasyonu ile sentezlenmiştir. Potasyum persulfat (KPS) başlatıcı olarak ve dodesilbenzen sülfonik asit (DBSA) yüzey aktif madde olarak kullanılmıştır. Monomerlerin toplam mol sayısı 0.075 olarak alınmıştır. MMA ve AN oda sıcaklığında 80 ml suya eklenmiştir. Ortam devamlı karıştırılarak monomerlerin çok küçük parçacıklar halinde dağılarak elde edilmesi sağlanmıştır. Daha sonra DBSA (yüzey aktif madde) ve KPS (başlatıcı) 40^{o}C'de eklenmiştir. Ortamda su, monomer, misel yapıcı ve başlatıcı bulunmaktadır. Monomerler yüzey aktif madde (DBSA) ile kararlı hale getirilmiştir ve miseller oluşmuştur. Emülsiyon polimerizasyonu 70^{o}C'de, 2 saat boşunca devamlı karıştırılarak devam etmiştir. FTIR-ATR kopolimer spektrumu, metil metakrilat için karakteristik pik olan C=O 1739 cm^{-1}'ye, akrilonitril için karakteristik pik olan C≡N 2242 cm^{-1}'ye kaydığını göstermiştir. Ayrıca 1639 cm^{-1}'de olan C=C çift bağın yok olduğu görülmektedir. Bu kopolimerin oluşumunun bir kanıtı olmuştur.

Poli(MMA-ko-AN) matriksi kullanılarak bunların Py, NMPy ve NPhPy içeren kompozitleri, kimyasal polimerizasyon (matriks polimerizasyonu) yöntemi ile serik amonyum nitrat başlatıcısı varlığında hazırlanmıştır. Kompozit yapılar, film dökme yöntemi ile filmler halinde, elektro-çekim yöntemi kullanılarak ise nanolifler halinde üretilmiştir. FTIR-ATR spektrofotometrik analizleri, 1250-1400 cm^{-1} arasındaki geniş bant aralığı, PPy türevlerine ait CH ve/veya CN düzlem içi deformasyon piklerini göstermiştir. 1436 cm^{-1} dalga sayısında görülen pik, PPy türevlerine ait CN halka titreşim pikidir. Kompozit film yapısına katılan Py türevi miktarının arttığı durumlarda 1436 cm^{-1} dalga sayısında görülen pikin absorbans değerlerinde de artışlar görülmüştür. Bu ilişki, P(MMA-ko-AN) ve PPy türevi fonksiyonel grupları arasında etkileşim olduğunu göstermiştir. Ayrıca, PPy türevine ait CH düzlem içi titreşimi (1312 cm^{-1}) olarak adlandırılan yeni bir absorpsiyon bandı gözlenmiştir.

PPy türevi içeren kompozit çözeltilerin UV-vis deneyleri, DMF referans alınarak gerçekleştirilmiştir. Buna göre, çözeltide PPy türevi bulunmadığı durumda UV-Vis spektrumunda herhangi bir pik gözlenmemiş iken, PPy bulunduğu durumda ise 462 nm civarında kuvvetli bir pik gözlenmiştir. Çözelti içerisindeki PPy miktarı arttıkça UV-Vis den elde edilen pikin absorbans değerleri de artş göstermiştir.

P(MMA-ko-AN)'nin iyi mekanik özellikleri ile PPy ve türevlerinin elektriksel özelliklerinin birleştirildiği yarı iletken kompozitler üretilmiştir. Ce(IV) ilk defa P(MMA-ko-AN) matriksi içerisinde Py ve türevlerini polimerleştirmek için kullanılmıştır. Ce(IV)'nin yüksek oksitleme yeteneği ve P(MMA-ko-AN) ile PPy türevleri fonksiyonel grupları arasındaki etkileşimden dolayı iletken polimerik tanecikler, matriks içerisinde homojen bir şekilde dağılım göstermiştir.

Matriks polimerizasyonu ile hazırlanan kompozit çözeltilerden ilk defa elektro-çekim yöntemi kullanılarak P(MMA-ko-AN)-PPy türevi kompozit nanolifleri üretilmiştir. Üretilen kompozitlerin spektroskopik (FTIR-ATR, UV-Vis), morfolojik (SEM), dielektrik/elektrik (Geniş bant dielektrik spektroskopisi) ve termal (DSC) karakterizasyonları gerçekleştirilmiştir.

1. INTRODUCTION

Conducting polymers can exhibit significant levels of electrical conductivity suitable for use in electronic devices, batteries, antistatic coatings, electromagnetic interference (EMI) shielding, electrochromic devices, optical switching devices, sensors, and so on [1]. Among those conducting polymers, polypyrrole is especially promising for commercial applications because of its good environmental investistability, facile synthesis, and higher conductivity than many other conducting polymers [2]. In general, conducting polymers themselves possess poor mechanical properties, for example, brittleness and poor processability. These drawbacks can be overcome, however, by forming blends or composites with other polymer matrices with good tractability [3]. The composite formation is one of the simplest methods for providing the processability of a conducting polymer. However, a conducting polymer exhibits poor compatibility with common polymers due to chain rigidity originated from an extended conjugate double bond. In the case of a conducting composite prepared by the simple coating of conducting polymers onto the surface of the matrix polymer, any interaction between the two components usually does not exist and the conducting polymer can be easily removed from the matrix polymer by repeated friction to result in the ultimate failure of the electrical property. In this regard, it should be stressed that the interaction between the two components should exist in order to provide the desirable properties [4]. The preparation of conducting composites/blends/films with the conventional vinyl polymers, like polyacrylonitrile (PAN), poly(methyl methacrylate) (PMMA), polystyrene (PS), polyacrylamide (PAA), and polyvinylchloride (PVC), have been attempted using several methods. The preparation of conducting polymeric blends/composites of PPy-PVC and PPy-PMMA using electrochemical and oxidative polymerization methods were also reported by several groups. Stanke and coworkers synthesized a conducting graft copolymer film of PMMA and PPy through the oxidative polymerization of Py with $FeCl_3$ [5]. Polymer composites of PAN/PPy, P(AN-co-AA)/PPy and P(AN-co-SS)/PPy were synthesized by impregnating pyrrole monomer into the matrix

followed by the polymerization of pyrrole in the matrix film. Anionic moieties supplied better electrostatic interaction between the polymer matrix and conducting polymer resulting better electrical properties as polymeric matrix roled as polymeric dopant [6]. A combination of conventional polymers or copolymers with conductive polymers allows the creation of new polymeric materials with interesting electrical properties [7]. The first poly(methyl methacrylate)/polypyrrole (PMMA/PPy) composite films with a conductivity of about 0.12 S cm^{-1} were reported by Morita et al. (1988) [8]. The electrical conductivity both dc and ac of polypyrrole doped with β-naphthalenesulfonicacid (NSA) and polypyrrole–polymethyl methacrylate blends were investigated in the literature [9]. Electromagnetic interference (EMI) shielding has crucial importance on electronic and communication industries [10]. Conducting polymers are suitable materials for eliminating EMI due to their high values of conductivity and dielectric permittivity as compared with other polymers. Not only they are lightweight, but also more flexible than metals and do not corrode [11].

In this study, influence of conjugated polymer on AC electrical conductivity and dielectric properties of P(MMA-co-AN) composite films were investigated, while polypyrrole (PPy), poly(N-Methyl Pyrrole) (PNMPy) and poly(N-phenylpyrrole) (PNPhPy) were used as conductive polymers. P(MMA-co-AN), which was used as matrix in composite film formation, was synthesized by oxidative copolymerization of MMA and AN monomers in aqueous medium. Afterwards, pyrrole (Py), N-Methyl Pyrrole (NMPy) and N-phenylpyrrole (NPhPy) were polymerized on P(MMA-co-AN) matrix in dimethylformamide (DMF). Ce(IV) salt was used as an oxidant for both copolymer formation and in-situ matrix polymerization due its strong oxidizing power. Composite films were then acquired by partially evaporation of DMF. Spectroscopic, electrical and thermal properties of thin films were analyzed. Also, nanofibers of P(MMA-co-AN) and in-situ polymerized pyrrole (Py), N-Methyl Pyrrole (NMPy) and N-phenyl pyrrole (NPhPy) on P(MMA-co-AN) matrix were acquired by electrospinning method. Spectroscopic and morphological properties of nanofibers were investigated.

2. THEORETICAL PART

2.1 History of Conducting Polymers

Polymers have always been considered as insulators of electricity. But now polymers could conduct as good as metals. This has been achieved through simple modification of ordinary organic conjugated polymers [12]. The term conjugated polymer defines a backbone chain that is unsaturated and therefore has alternating double and single bonds along the chain, all carbon atoms are singly bonded to neighboring carbon atoms and remaining valence electrons are bound to hydrogen atoms. Conjugated polymers can be converted into metals by doping and therefore form new class of materials referred as synthetic metals, or conducting polymers [13].

The intrinsic ability of certain polymers to conduct electricity has been known for some time; it was discovered as far back as 1862 when Letheby produced a partly conductive material by the anodic oxidation of aniline in a sulfuric acid solution, which in all likelihood was polyaniline. Polypyrrole was discovered in the 1960s, but little was understood about the mechanism of its electrical conduction, and this knowledge was essentially lost. Polyacetylene was the first conductive polymer to be fully explored and understood and led to an increasing interest in this field. While Natta and colleagues were the first to prepare this polymer in 1958, their work was not widely recognized. A new synthetic procedure developed by Shirakawa allowed the controlled production of nearly allecis-polyacetylene or all-trans-polyacetylene, though these materials still possessed relatively modest conductivity in the order of 10^{-1} to 10^{-7} S/m. In 1976 Shirakawa, Professors Heeger and MacDiarmid used their knowledge regarding to further explore the doping of polyacetylene. An iodine doped all-trans-polyacetylene was produced with a conductivity of 3000 S/m, a vast improvement over the undoped form. Further experimentation with both the cis and trans forms led to the creation of doped polyacetylene with conductivity up to eleven orders of magnitude larger than the undoped state. These findings fostered a heightened interest in conducting polymers and the many potential applications in

which they could be employed, leading to Shirakawa, Heeger, and MacDiarmid being awarded the Nobel Prize in Chemistry in 2000 [14].

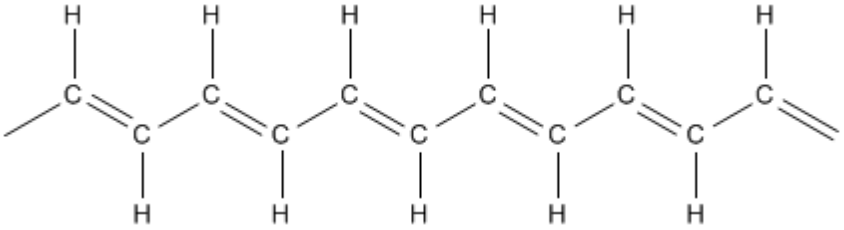

Figure 2.1 : Molecular structure of polyacetylene.

The discovery of highly conducting polyacetylene led to a sudden spurt in research activity directed towards the study of new conducting polymeric systems. The instability of polyacetylene in air further intensified this research. The result is that at present many novel conducting systems are known and these include polypyrrole, poly(phenylacetylene),poly(p-phenylenesulphide),poly(p-phenylene),polythiophene, polyfuran, polyaniline, polyisothianaphthene and their derivatives [12].

2.2 Application of Conducting Polymers

There are two main groups of applications for these polymers. The first group utilizes their conductivity as its main property. The second group utilizes their electroactivity. The extended π-systems of conjugated polymer are highly susceptible to chemical or electrochemical oxidation or reduction. These alter the electrical and optical properties of the polymer, and by controlling this oxidation and reduction, it is possible to precisely control these properties. Since these reactions are often reversible, it is possible to systematically control the electrical and optical properties with a great deal of precision. It is even possible to switch from a conducting state to an insulating state. The two groups of applications are shown below:

Group 1:

Electrostatic materials, conducting adhesives, electromagnetic shielding, printed circuit boards, artificial nerves, antistatic clothing, piezoceramics, active electronics (diodes, transistors), aircraft structures.

Group 2:

Molecular electronics, electrical displays, chemical-biochemical and thermal sensors, rechargeable batteries and solid electrolytes, drug release systems, optical computers, ion exchange membranes, electromechanical actuators, smart structures, switches.

Group 1-Conductivity:

These applications uses just the polymer's conductivity. The polymers are used because of either their light weight, biological compatibility for ease of manufacturing or cost.

By coating an insulator with a very thin layer of conducting polymer it is possible to prevent the buildup of static electricity. This is particularly important where such a discharge is undesirable. Such a discharge can be dangerous in an environment with flammable gasses and liquids and also in the explosives industry. In the computer industry the sudden discharge of static electricity can damage microcircuits. This has become particularly acute in recent years with the development of modern integrated circuits. To increase speed and reduce power consumption, junctions and connecting lines are finer and closer together. The resulting integrated circuits are more sensitive and can be easily damaged by static discharge at a very low voltage. By modifying the thermoplastic used by adding a conducting plastic into the resin results in a plastic that can be used for the protection against electrostatic discharge [15].

By placing monomer between two conducting surfaces and allowing it to polymerise it is possible to stick them together. This is a conductive adhesive and is used to stick conducting objects together and allow an electric current to pass through them.

Many electrical devices, particularly computers, generate electromagnetic radiation, often radio and microwave frequencies. This can cause malfunctions in nearby electrical devices. The plastic casing used in many of these devices are transparent to such radiation. By coating the inside of the plastic casing with a conductive surface this radiation can be absorbed. This can best be achieved by using conducting plastics. This is cheap, easy to apply and can be used with a wide range of resins. The final finish generally has good adhesion, gives a good coverage, thermally expands approximately the same as the polymer it is coating, needs just one step and gives a good thickness [16] .

Many electrical appliances use printed circuit boards. These are copper coated epoxy-resins. The copper is selectively etched to produce conducting lines used to connect various devices. These devices are placed in holes cut into the resin. In order to get a good connection the holes need to be lined with a conductor. Copper has been used but the coating method, electroless copper plating, has several problems. It is an expensive multistage process, the copper plating is not very selective and the adhesion is generally poor. This process is being replaced by the polymerisation of a conducting plastic. If the board is etched with potassium permanganate solution a thin layer of manganese dioxide is produced only on the surface of the resin. This will then initiate polymerisation of a suitable monomer to produce a layer of conducting polymer. This is much cheaper, easy and quick to do, is very selective and has good adhesion [17] .

Due to the biocompatability of some conducting polymers they may be used to transport small electrical signals through the body, i.e. act as artificial nerves. Perhaps modifications to the brain might eventually be contemplated [18].

Weight is at a premium for aircraft and spacecraft. The use of polymers with a density of about 1 g cm^{-1} rather than 10 g cm^{-1} for metals is attractive. Moreover, the power ratio of the internal combustion engine is about 676.6 watts per kilogramme. This compares to 33.8 watts per kilogramme for a battery-electric motor combination. A drop in magnitude of weight could give similar ratios to the internal combustion engine [18]. Modern planes are often made with light weight composites. This makes them vulnerable to damage from lightning bolts. By coating aircraft with a conducting polymer the electricity can be directed away from the vulnerable internals of the aircraft.

Group 2-Electroactivity:

Depending on the conducting polymer chosen, the doped and undoped states can be either colourless or intensely coloured. However, the colour of the doped state is greatly redshifted from that of the undoped state. The colour of this state can be altered by using dopant ions that absorb in visible light. Because conducting polymers are intensely coloured, only a very thin layer is required for devices with a high contrast and large viewing angle.

Unlike liquid crystal displays, the image formed by redox of a conducting polymer can have a high stability even in the absence of an applied field. The switching time achieved with such systems has been as low as 100 μs but a time of about 2 ms is more common. The cycle lifetime is generally about 10^6 cycles. Experiments are being done to try to increase cycle lifetime to above 10^7 cycles [19].

The chemical properties of conducting polymers make them very useful for use in sensors. This utilizes the ability of such materials to change their electrical properties during reaction with various redox agents (dopants) or via their instability to moisture and heat. An example of this is the development of gas sensors. It has been shown that polypyrrole behaves as a quasi 'p' type material. Its resistance increases in the presence of a reducing gas such as ammonia, and decreases in the presence of an oxidizing gas such as nitrogen dioxide. The gases cause a change in the near surface charge carrier (here electron holes) density by reacting with surface adsorbed oxygen ions [20]. Another type of sensor developed is abiosensor. This utilizes the ability of triiodide to oxidize polyacetylene as a means to measure glucose concentration. Glucose is oxidized with oxygen with the help of glucose oxidase. This produces hydrogen peroxide which oxidizes iodide ions to form triiodide ions. Hence, conductivity is proportional to the peroxide concentration which is proportional to the glucose concentration.

Probably the most publicized and promising of the current applications are light weight rechargeable batteries. Some prototype cells are comparable to, or better than nickel-cadmium cells now on the market. The polymer battery, such as a polypyrrole-lithium cell operates by the oxidation and reduction of the polymer backbone. During charging the polymer oxidizes anions in the electrolyte enter the porous polymer to balance the charge created. Simultaneously, lithium ions in electrolyte are electrodeposited at the lithium surface. During discharging electrons are removed from the lithium, causing lithium ions to reenter the electrolyte and to

pass through the load and into the oxidized polymer. The positive sites on the polymer are reduced, releasing the charge-balancing anions back to the electrolyte. This process can be repeated about as often as a typical secondary battery cell [15,16].

Conducting polymers can be used to directly convert electrical energy into mechanical energy. This utilizes large changes in size undergone during the doping and dedoping of many conducting polymers. This can be as large as 10%. Electrochemical actuators can function by using changes in a dimension of a conducting polymer, changes in the relative dimensions of a conducting polymer and a counter electrode and changes in total volume of a conducting polymer electrode, electrolyte and counter electrode. The method of doping and dedoping is very similar as that used in rechargeable batteries discussed above. What is required are the anodic strip and the cathodic strip changing size at different rates during charging and discharging. The applications of this include microtweezers, microvalves, micropositioners for microscopic optical elements, and actuators for micromechanical sorting (such as the sorting of biological cells).

One of the most futuristic applications for conducting polymers are 'smart' structures. These are items which alter themselves to make themselves better. An example is a golf club which adapt in real time to a persons tendency to slice or undercut their shots. A more realizable application is vibration control. Smart skis have recently been developed which do not vibrate during skiing. This is achieved by using the force of the vibration to apply a force opposite to the vibration. Other applications of smart structures include active suspension systems on cars, trucks and train; traffic control in tunnels and on roads and bridges; damage assessment onboats; automatic damping of buildings and programmable floors for robotics [19].

2.3 Conduction Mechanism in Conducting Polymers

2.3.1 Band theory

The conducting polymers are a class of organic semiconductors having a negative temperature coefficient of conductivity and hence the theory of the conventional semiconductors was used to discuss the conduction mechanism. A key requirement for a polymer to become intrinsically conducting is that there should be overlap of molecular orbitals to allow the formation of delocalized molecular wave functions. Besides this molecular orbitals must be partially filled, so that there is free movement of electrons throughout the lattice [21]. In the band theory, the atomic orbitals of

each atom overlap with the same orbitals of their neighborhood atoms in all directions to produce molecular orbitals similar to those in small molecules.

When these orbitals are spaced together in a given range of energies, they form what looks like continuous energy bands. The electrical properties of conventional inorganic semiconducting materials depend on the band structure. When the bands are filled or empty, no conduction occurs. If the band gap is narrow, at room temperature, thermal excitation of electrons from the valence band to the conduction band gives rise to conductivity. This is what happens in classical semiconductors. When the band gap is too wide, thermal excitation at room temperature is insufficient to excite electrons across the gap and the solid is an insulator. The high conductivity of metals is due to partially occupied bands, a partially filled conduction band, a partially empty valence band, or a zero band gap.

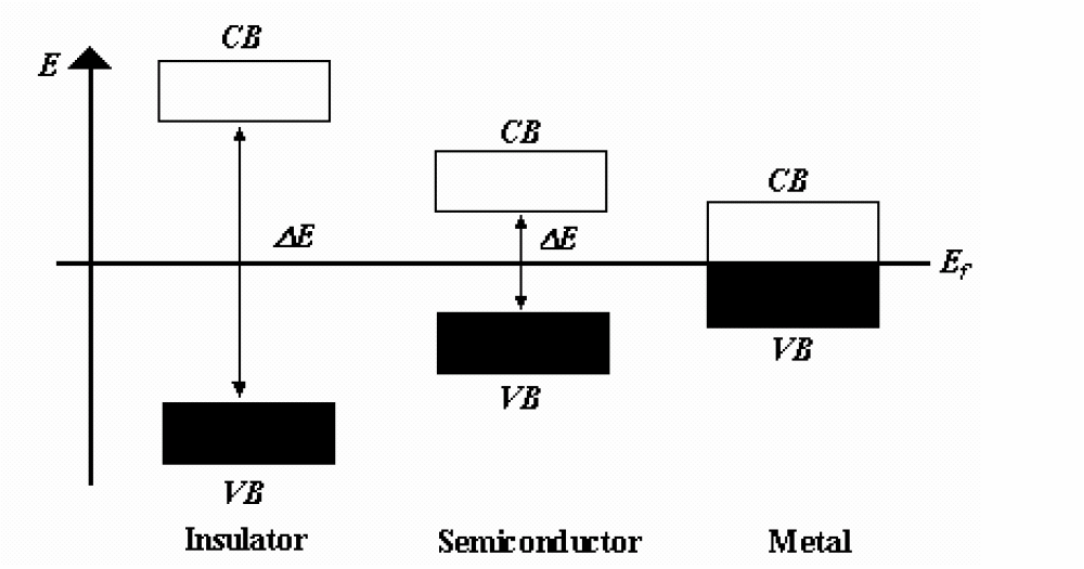

Figure 2.2 : Energy band in solid.

2.3.2 Charge carriers

In order to induce high electrical conductivity in organic conjugated polymers, charge carriers must be introduced. These charge carriers are created by removing electrons from, or adding electrons to, the delocalized p-electron network of the polymer, creating a conducting unit that is now a polymeric ion rather than a neutral species. The charges introduced are compensated by ions from the reaction medium.

This process is called doping by analogy to the changes that occur in inorganic semiconductors upon addition of small quantities of electronic defects.

However, it proceeds through a different mechanism and is more precisely termed a redox reaction [22,23]. The ability to control the electrical properties of conducting polymers over wide ranges, by adjusting the redox doping level, has created interest in these materials for a number of emerging applications [24].

Metals have unpaired electrons and their highest occupied electronic levels are half-occupied. Electrical conductivity results from the fact that the electrons can move readily under an electric field since there is no forbidden gap between the highest occupied and lowest unoccupied electronic levels. Conductivity is limited, therefore, by defects in the lattice and vibrational distortions (also called phonons). Since this phonon activity increases with elevated temperatures, the conductivity of metals increases as the temperature is decreased. However, the electrons in conjugated organic polymers, as in inorganic semiconductors, are paired, creating a gap between the highest occupied levels (the valence band) and the lowest unoccupied levels (the conduction band). The energy difference between these bands gives rise to the intrinsic insulating or semiconducting properties of conjugated organic polymers. The moderate conductivity of these materials is a result of thermal excitation of valence electrons into the conduction band. Therefore, the conductivity of semiconductors and conjugated organic polymers increases with increasing temperature in the neutral or undoped state. The mechanism for the conductivity increase resulting from doping in inorganic semiconductors involves the formation of unfilled electronic bands. Electrons are removed from the top of the valence band during oxidation, called p-type doping, or added to the bottom of the conduction band during reduction, termed n-type doping.

Extension of this argument to the case of conjugated organic polymers was found to be inaccurate as the conductivity in many conducting polymers was found to be associated with spinless charge carriers.

In situ electron spin (epr)/electrochemistry techniques have shown that the conducting entity in polyacetylene, polypyrrole, polythiophene, and poly(p-phenylene) can be spinless, although evidence exists for mixedvalence charge carriers as well.

The conductivity increase following doping in conjugated polymers is explained in terms of local lattice distortions and localized electronic states. In this case, the valence band remains full and the conduction band remains empty so that there is no appearance of metallic character. When the polymer chain is redox doped, a lattice distortion results and the equilibrium geometry for the doped state is different than the ground-state geometry. This is evident in many small organic molecules, eg, the ground-state geometry of biphenyl is benzenoid but the geometry of its radical cation is quinoidal.

Many conjugated polymers have nondegenerate ground states that behave similarly upon redox doping. When one electron is removed (or added) to the polymer chain a radical cation (or anion) is formed. This results in a lattice distortion that leads to an upward shift of the highest occupied molecular orbital (HOMO) and a downward shift in the lowest unoccupied molecular orbital (LUMO). Although the radical ion is expected to be delocalized over the entire polymer chain, the species is localized, with a localized lattice distortion creating a localized electronic state. Since the geometry of the chain between the radical and the ion must be distorted, and the energy of the distorted geometry is normally higher than that of the ground state, separation, and delocalization of the radical ion results in energetically unfavorable further lattice distortions. This radical ion associated with a lattice distortion is called a polaron as shown in Figure 2.3 for PPP. A similar argument can be used when a second electron is removed from (or added to) this site. The resulting species is a dication (or dianion), with a lattice distortion separating the two charges. This species is termed a bipolaron and is also illustrated in Figure 2.3 [25].

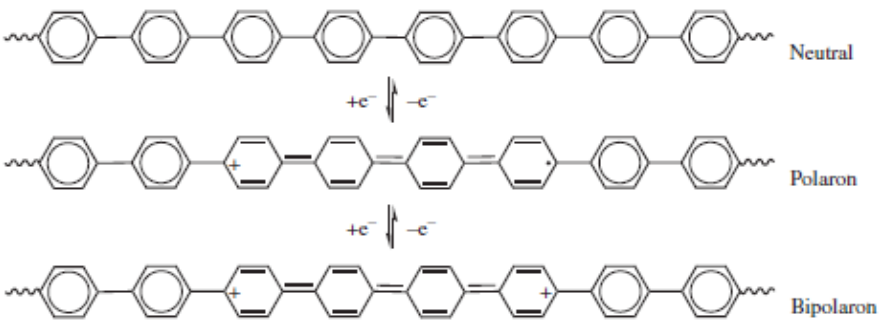

Figure 2.3 : Lattice distortions in poly(*p*-phenylene) [25].

At higher doping levels, the polarons are replaced with bipolarons. The bipolarons are located symmetrically with a band gap of 0.75 eV for polypyrrole. This, eventually, with continued doping, forms into a continuous bipolaron bands. Their band gap also increases as newly formed bipolarons are made at the expense of the band edges. For a very heavily doped polymer, it is conceivable that the upper and the lower bipolaron bands will merge with the conduction and the valence bands, respectively, to produce partially filled bands and metallic conductivity. This is shown in Figure 2.4 [26].

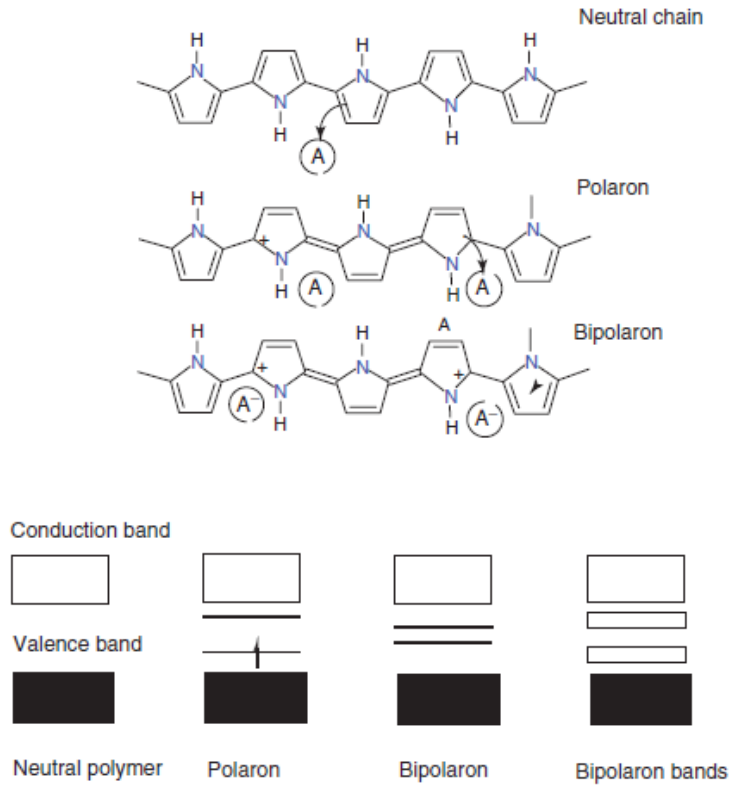

Figure 2.4 : Mechanism of conduction on polymer doping [26].

2.3.3 Doping process

During the doping process, an organic polymer, either an insulator or a semiconductor having a small conductivity, typically in the range 10^{-10}–10^{-5} S/cm, is converted into a polymer, which is in the "metallic" conducting regime (circa 1–10^{4} S/cm). The controlled addition of known, usually small (≤10%), nonstoichiometric quantities of chemical species results in significant changes in the electronic, electrical, magnetic, optical, and structural properties of the polymer.

Doping is reversible to produce the original polymer with little or no degradation of the polymer backbone. Both doping and undoping processes, involving dopant counterions that stabilize the doped state, may be carried out chemically or electrochemically.

All conducting polymers (and most of their derivatives), for example, poly(paraphenylene), poly(phenylene vinylene), polypyrrole, polythiophene (PT), polyfuran, poly(heteroaromatic vinylenes), and polyaniline, undergo p- and/or n-redox doping.

p-Doping, that is, partial oxidation of the *p* backbone of an organic polymer, was first discovered by treating *trans*-$(CH)_x$ with an oxidizing agent such as iodine:

$$\textit{trans}\text{-}(CH)_x + 1.5xyI_2 \rightarrow [(CH^{)+y}\ (I_3)^-_y]_x,\ y \leq 0.07 \qquad \textbf{(2.1)}$$

This process was accompanied by an increase in conductivity from circa 10^{-5} to circa 10^3 S/cm. If the polymer is stretch-oriented five- to sixfold before doping, conductivities parallel to the direction of stretching up to about 10^5 S/cm can be obtained.

p-Doping can also be accomplished by electrochemical anodic oxidation by immersing a *trans*-$(CH)_x$ film in, for example, a solution of LiClO4 dissolved in propylene carbonate and attaching it to the positive terminal of a DC (direct current) power source, the negative terminal being attached to an electrode also immersed in the solution:

$$\textit{trans}\text{-}(CH)_x + (xy)\ (ClO_4)^- \rightarrow [(CH)^{+y}\ (ClO_4)^{y-}]_x + (xy)\ e^-,\ y \leq 0.1 \qquad \textbf{(2.2)}$$

n-Doping, that is, partial reduction of the backbone p-system of an organic polymer, was also discovered using *trans*-(CH)*x* by treating it with a reducing agent such as liquid sodium amalgam or preferably sodium naphthalene (Nphth):

$$\textit{trans}\text{-}(CH)_x + (xy)\ Na^+(Nphth)^- \rightarrow [(CH)^{-y}\ Na_y^+]_x + Nphth,\ y \leq 0.1 \qquad \textbf{(2.3)}$$

The antibonding π-system is partially populated by this process, which is accompanied by an increase in conductivity of about 10^3 S/cm. n-Doping can also be carried out by electrochemical cathodic, by immersing a *trans*-$(CH)_x$ film in, for example, a solution of LiClO, dissolved in tetrahydrofuran and attaching it to the negative terminal of a DC power source, the positive terminal being attached to an electrode also immersed in the solution:

$$\textit{trans}\text{-}(CH)_x + (xy)\ Li^+ + (xy)\ e^- \rightarrow [(CH)^{-y}\ Li_y^+]_x,\ y \leq 0.1 \quad \textbf{(2.4)}$$

In all chemical and electrochemical p- and n-doping processes discovered for $(CH)_x$ and for the analogous processes in other conducting polymers, counter "dopant" ions are introduced, which stabilize the charge on the polymer backbone [26].

2.3.4 Hopping process

The conduction process can be described with two important mechanisms, doping and hopping. Hopping is simply intra-chain, inter-chain and inter-particle motion of charges in a polymer matrix [27]. The intra-chain movement, motion of the charge carrier through a single chain, depends on the efficient conjugation. On the other hand, inter-chain movement, jumping from one chain to another, is determined by the piling of the polymer chains. The mobility also depends on the movement of electrical charges from particle to particle.

Variable range hopping process in which electrons are delocalized on monomer rings is a well described conductivity mechanism. This mechanism, which is known as hopping conduction, is observed in two well-known varieties, nearest neighbor hopping and variable range hopping. The latter conduction mechanism is distinguishable from other conduction mechanisms by its different temperature dependence:

$$\sigma = \sigma^0 \exp\left[-(T_o/T)^{\gamma}\right] \quad \textbf{(2.5)}$$

γ depends on the dimensionality of the hopping process [28].

To sum up, the mobility and therefore conductivity are determined on both a macroscopic (inter-particle) and microscopic (intra- and inter-chain) levels.

2.4 Composites

A composite is defined as a material created by combination of two or more components namely, a selected filler or reinforcing agent and a compatible matrix binder. The combination of these component results in formation of a new material with specific characteristics and properties. The synthetic assemblage of the components does not occur as a dissolvation but rather like merging into each other to act in concert. Although the components act together as a single material, both the

components and the interface between them can usually be physically identified. Genarally, the behaviour and the properties of the composite is controlled by the interface of the components. Since the composite is a totally new material having new and specific characteristics, its properties cannot be achieved by any of its components acting alone.

The classification of composites can be done in different ways. The composites can be classified on the basis of the form of their structural components: fibrous where the composite is composed of fibers in a matrix, laminar where the composite is composed of layers in a matrix, and particulate where the composite is composed of particles in a matrix [29].

Another type of classification can be done on the basis of filler or reinforcing agent used namely polymer matrix composites, metal matrix composites, ceramic matrix composites, carbon-carbon matrix composites, intermetallic composites, or hybrid composites [30].

2.4.1 Polymer matrix composites

Composite materials have been utilized to solve technological problems for a long time. In 1960s with the introduction of polymeric-based composites, composites start capturing the attention of industries. Since then, composite materials have become common engineering materials. They are designed and manufactured for various applications including automotive components, sporting goods, aerospace parts, consumer goods, and in the marine and oil industries. Increasing awareness of product performance and competition in the global market for lightweight components also supported the growth in composite usage. Among all materials, composite materials have the potential to replace widely used steel and aluminum, and many times with better performance.

Replacing steel components with composite components can save 60 to 80% in component weight, and 20 to 50% weight by replacing aluminum parts. Today, it appears that composites are the materials of choice for many engineering applications. The matrix material used in polymer-based composites can either be

thermoset (epoxies, phenolics) or thermoplastic resins (low density polyethylene, high density polyethylene, polypropylene, nylon, acrylics). The filler or reinforcing agent can be choosen according to the desired properties. The properties of polymer matrix composites are determined by properties, orientation and concentration of fibers and properties of matrix.

The matrix has various functions such as providing rigidity, shaping the structure by transfering the load to fiber, isolating the fiber to stop or slow the propagation of crack, providing protection to reinforcing fibers against chemical attack and mechanical damage (wear), and affecting the performance characteristics such as ductility, impact strength, etc. depending on its type. The failure mode is strongly affected by the type of matrix material used in the composite as well as its compatibility with the fiber. The important functions of fibers include carrying the load, providing stiffness, strength, thermal stability, and other structural properties in the composites and providing electrical conductivity or insulation, depending on the type of fiber used [31].

2.4.2 Nanocomposites

Nanocomposites can be defined as multiphase materials where one or more of the phases have at least one dimension of order 100 nm or less. Most nanocomposites that have been developed and that have demonstrated technological importance have been composed of two phases, and can be microstructurally classified into three principal types: (a) Nanolayered composites composed of alternating layers of nanoscale dimension; (b) nanofilamentary composites composed of a matrix with embedded (and generally aligned) nanoscale diameter filaments; (c) nanoparticulate composites composed of a matrix with embedded nanoscale particles. As with conventional composites, the properties of nanocomposites can display synergistic improvements over those of the component phases individually. However, by reducing the physical dimension(s) of the phase(s) down to the nanometer length scale, unusual and often enhanced properties can be realized. An important microstructural feature of nanocomposites is their large ratio of interphase surface area to volume. For example, in dispersions of layered clay (aluminosilicates) in nanocomposite polymers, this ratio can approach 700 m^2/cm^3 which is of order the area of a football field within the volume of a raindrop. This large surface area can

result in novel and often enhanced properties that can be exploited technologically. In terms of their engineering applications, nanocomposites can be classified either as functional materials (based on their electrical, magnetic, and/or optical behavior) or as structural materials (based on their mechanical properties) [32].

Polymer-based nanocomposites for structural and functional material applications have received a great deal of recent attention. In terms of commercial importance, structural nanocomposites produced using layered clay minerals, such as montmorilonite and hectorite are the most significant. The layered clay (aluminosilicates) materials are synthesized by mixing the layered clay with the monomer, followed by polymerization, by melt mixing the layered clay with the polymer, or by mixing the layered clay with a solvated polymer followed by solvent removal. Another type of commercially important nanocomposite are thermoplastics reinforced with carbon nanotubes formed by extrusion and injection molding. The high modulus and tensile strength of carbon nanotubes make them extremely attractive filler materials for nanocomposite polymers [32].

2.5 Polypyrrole

Among the conducting polymers, polypyrrole (PPy) is especially promising for commercial applications because of its good environmental stability, facile synthesis, and higher conductivity than many other conducting polymers. PPy can often be used as biosensors, gas sensors, wires, microactuators, antielectrostatic coatings, solid electrolytic capacitor, electrochromic windows and displays, and packaging, polymeric batteries, electronic devices and functional membranes, etc. PPy can be easily prepared by either an oxidatively chemical or electrochemical polymerization of pyrrole. However synthetically conductive PPy is insoluble and infusible, which restricts its processing and applications in other fields.

The problem has been extensively investigated and new application fields have also been explored in the past several years. For example, PPy-based polymers can be used to load and release drugs and biomolecules.

PPy-based polymer blends can protect the corrosion of metals. Because of the strong adhesion of PPy to iron or steel treated with nitric acid, PPy polymers can be used as good adhesives. In a recent report, PPy-modified tips for functional group

recognition are applied in scanning tunneling microscopy [33].

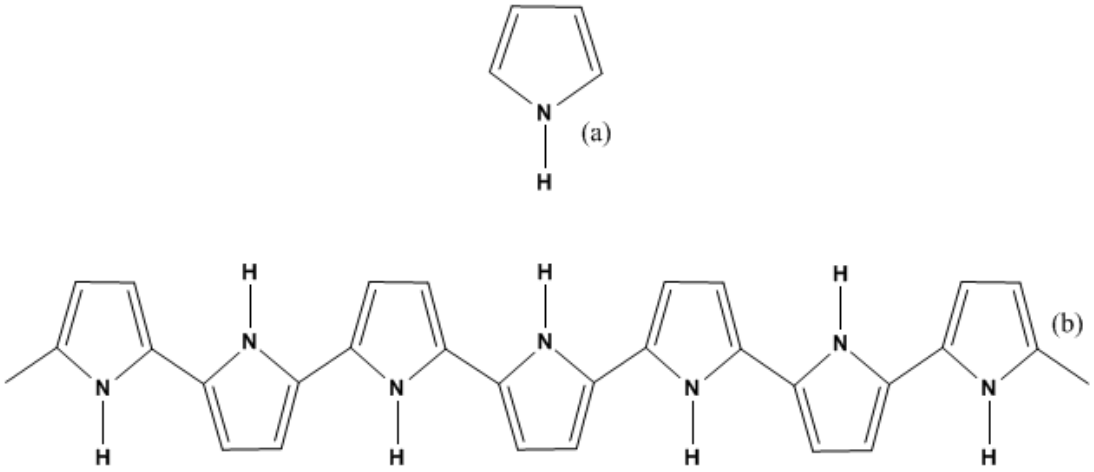

Figure 2.5 : Chemical structure of (a) pyrrole and (b) polypyrrole.

2.5.1 Synthesis of polypyrrole

Polypyrrole and many of its derivatives can be synthesized via simple chemical or electrochemical methods [34]. Photochemically initiated and enzyme-catalyzed polymerization routes have also been descibed but less developed. Different synthesis routes produce polypyrrole with different forms; chemical oxidations generally produce powders, while electrochemical synthesis leads to films deposited on the working electrode and enzymatic polymerization gives aqueous dispersions [35].

As mentioned above the electrochemical polymerization method is utilized extensively for production of electroactive/conductive films. The film properties can be easily controlled by simply varying the electrolysis conditions such as electrode potential, current density, solvent, and electrolyte. It also enables control of thickness of the polymers.

Electrochemical synthesis of polymers is a complex process and various factors such as the nature and concentration of monomer/electrolyte, cell conditions, the solvent, electrode, applied potential and temperature, pH affects the yield and the quality of the film. Thus, optimization of all of the parameters in one experiment is difficult.

In contrast, chemical polymerization does not require any special instruments, it is a rather simple and fast process. Chemical polymerization method involves oxidative polymerization of pyrrole monomer by chemical oxidants either in aqueous or non-aqueous solvents or oxidation by chemical vapour deposition in order to produce bulk polypyrrole as fine powders [36].

Iron (III) chloride and water are found to be the best oxidant and solvent for chemical polymerization of pyrrole respectively regarding desirable conductivity characteristics.

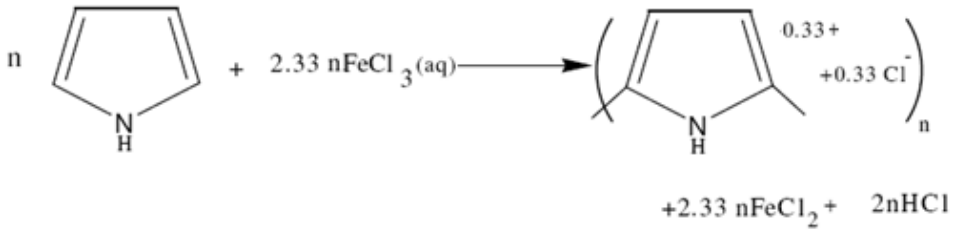

Figure 2.6 : Chemical polymerization of polypyrrole.

Previous studies have shown that the optimum initial mole ratio of Fe(III)/Pyrrole for polymerization by aqueous iron (III) chloride solution at 19˚C is 2,25 or 2,33. Also, several studies have revealed that factor such as solvent, reaction temperature, time, nature and concentration of oxidizing agent, affect the oxidation potential of the solution which affects the final conductivity of the product [36].

2.5.2 Composites of polypyrrole

The main disadvantages in PPy are poor thermal stability and poor processability in states of both melt and solution due to the nature of rigidity of its backbone. The rigidity of its chain originates from the presence of strong interchain interactions which greatly limits the application of PPy in many commercial fields.

Therefore, various approaches have been utilized to make PPy processable such as modification of PPy backbone, preparation of stable colloidal dispersion of PPy particles in an aqueous or non-aqueous medium, use of polymeric or surfactant-type dopant anions, and preparation of composites and nanocomposites [37].

Maria Omastova, Stanislav Kosina, Jürgen Pionteck, Andreas Janke and Juraj Pavlinec prepared conducting polymer composites of polyethylene and polypyrrole (PE/PPy) , polypropylene and polypyrrole(PP/PPy) , and poly (methyl methacrylate) and polypyrrole (PMMA/PPy) by means of a chemical modification method, resulting in a network-like structure of polypyrrole embedded in the insulating polymer matrix. Polyethylene (PE), polypropylene (PP) and poly (methyl methacrylate) (PMMA) particles were coated with PPy by the chemical polymerization method. The prepared powder composite samples PE/PPy, PP/PPY and PMMA/PPy were compression moulded. The conductivity of the compression-moulded samples was measured. Electrical conductivity of compression-moulded samples reached values from $1x10^{-11}$ to 1 S/cm. Large amount of material with good antistatic and conductive properties prepared in an inexpensive way using the method of chemically oxidative modification of PE, PP or PMMA particles by pyrrole. These conductive composites can find applications as antistatic packaging and as materials for electromagnetic radiation shielding [38].

Hua Bai , Lu Zhao , Canhui Lu , Chun Li and Gaoquan Shi prepared various conducting polymer/hydrophobic insulating polymer (CP/HIP) composite nanofibers by electrospinning and vapor deposition polymerization (VDP) with benzoyl peroxide (BPO) as oxidant. BPO is soluble in N,N-dimethylformamide (DMF) and can form homogenous solutions with hydrophobic polymers such as poly(methyl methacrylate) (PMMA) and polystyrene (PS). PMMA solution was prepared by dissolving in DMF. Then, a controlled amount of BPO was dissolved in the PMMA solution to prepare a BPO/PMMA blended solution. The blended solutions were electrospun at room temperature. Continuous nanofibers were deposited on the surfaces of counter electrodes and collected in the form of non-woven mats. To prepare PPy/HIP composite fibers, electrospun HIP fibers containing BPO were put into a reaction vessel equipped with an aqueous pyrrole solution and an aqueous hydrochloric acid solution loading reservoirs. The monomer and hydrogen chloride in the reservoirs evaporated gradually and diffused into the BPO/HIP composite fibers where the polymerization was occurred.

The nonwoven mats of the resulting CP/HIP composite fibers can be used as the high-sensitive sensing elements of gas sensors. A gas senor based on polypyrrole (PPy)/PMMA composite fibers was fabricated for sensing ammonia or chloroform

vapor, and exhibited greatly improved performances comparing with those of the device based on a PPy flat film [39].

Gaoyi Han and Gaoquan Shi were developed a simple method for preparing porous PPy/PMMA composite films by reacting pyrrole vapor with an organic ferric salt embedded in PMMA films. The ammonia sensors based on these composites were tested to have relatively high sensitivity and fast response. The ferric salt was prepared by reacting AOT with ferric chloride in distilled water. Various amounts of FeAOT were dissolved into chloroform solution of PMMA. The mixtures were cast onto glass slides. The FeAOT/PMMA films were placed into the pyrrole vapor. Then, the films were immersed in methanol to wash the resulted Fe^{2+}AOT. The mixtures of PMMA and various amounts of FeAOT were dropped onto stainless steel sheets to prepare of the electrodes coated with PPy/PMMA. The electrodes were treated with pyrrole vapors. Then the electrodes were washed with methanol. A simple resistance device based on this composite film was fabricated and applied to detect ammonia gas at room temperature. The sensitivity of the porous composite films towards ammonia was considerably higher than that of an electrochemically deposited PPy films. Furthermore, the response speed of the sensors was also fast. The porous PPy/PMMA composite films were one of the optima for fabricating sensitive and low-cost ammonia sensors [40].

Maziar Nikpour, Hassan Chaouk, Albert Mau, Dong Jun Chung and Gordon Wallace prepared a series of porous membranes consisting of polymethyl methacrylate (PMMA) and polypyrrole (PPy) using porogen leaching techniques. In this work two different approaches of obtaining controlled porosity conducting polymer composites were investigated. The first one was the use of a liquid porogen (polypropylene glycol). The second one the use of a solid porogen, sodium chloride. The membranes could be made to be permeable to small amino acids (tryptophan) or large proteins (BSA). The membranes demonstrated conductivities up to 19.8 S/cm and with further development may have applications in bioseparations and other areas that require controlled porosity conducting polymer composites [41].

W.S. Barde, S.V. Pakade and S.P. Yawale synthesized Polypyrrole (PPy) and poly (vinyl acetate) (PVAc) composite thin films by chemical oxidative polymerization method with the solution of ferric chloride ($FeCl_3$) oxidant in methanol. Their dc conductivities as a function of temperature ($308\text{-}383^0$ K) were measured. The ionic

transference numbers for the PPy-PVAc films, synthesized with different concentration of $FeCl_3$, were determined by dc polarization technique. The dc electrical conductivity of the films, at room temperature, first increases with concentration of $FeCl_3$ and attains the maximum value ($r = 6.17 \times 10^{-10}$ S/cm) at 0.5 M of $FeCl_3$ [42].

Polyacrylonitrile(PAN)/Polypyrrole(PPy) and its derivatives composite thin films were prepared by polymerization of pyrrole, N-methyl pyrrole and N-phenyl pyrrole respectively on polyacrylonitrile matrix. Effect of concentration of pyrrole derivatives on the resulting polymeric film properties was investigated. The influence of the pyrrole derivative type and content on the dielectric permittivity, dielectric loss and electrical properties of the composite films were analyzed in the frequency range from 0.05 Hz to 10 MHz. For a selected concentration of 200 μl of composite films at 10^7 Hz, the conductivity was found to be in the following order: PAN-PPy<PAN-PNMPy<PAN-PNPhPy. Dielectric constant increase of the composite films is more obvious when the quantity of n-phenyl pyrrole is increased [43].

2.6 Poly(Methyl methacrylate-co-Acrylonitrile)

Acrylonitrile copolymerizes readily with electron-donor monomers. Copolymerization is carried out by bulk emulsion, slurry or susupension processes. The arrangement of monomer units in acrylonitrile copolymers is most commonly random. Special techniques can be used to achieve specific arrangements.

Because of the combination of high melting point, high melt viscosity, and poor thermal stability, acrylonitrile homopolymer has little application. Even in synthetic fibers, small amounts of copolymers are incorporated to improve stability, dye receptivity and certain other properties. By copolymerizing acrylonitrile with other monomers, the deficiencies of acrylonitrile homopolymer have been tempered and at the same time the unusual and desirable properties of acrylonitrile have been incorporated into various melt-processible resins. For general applications, acrylonitrile content ranges up to ca 50%; for barrier applications, to ca 75%. Acrylonitrile copolymer properties, such as rigidity, chemical resistance, melt viscosity, stability, and permeability, generally vary in proportion to the acrylonitrile content. However, the glass-transition temparature (T_g) shows unusual behavior;

there is a maximum or a minimum T_g in certain cases, eg, for copolymers of styrene, vinylidene chloride, and methyl methacrylate.

Copolymers of acrylonitrile and methyl methacrylate and terpolymers of acrylonitrile, styrene and methyl methacrylate are used as barrier polymers. Acrylonitrile multi polymers contaaining methyl methacrylate, α-methyl styrene and indene are used as PVC modifiers to melt blend with PVC. These PVC modifiers not only enhance the heat distortion temperature, but also improve the processibility of the PVC compounds [44].

The poor comprehensive performance of the gel polymer electrolyte (GPE) for lithium ion battery with homopolymer as matrix can be improved to different extents by using copolymers from monomers with different functions. For example, the performance of the GPE with PMMA or PAN as matrix can be improved by using the copolymer of MMA and AN. A new copolymer, poly(methyl methacrylate-acrylonitrile-vinyl acetate) (P(MMA-AN-VAc)) is reported by employing the individuals advantages of three monomers, MMA, AN and vinyl acetate (VAc). AN provides the copolymer with good processability, electrochemical and thermal stability. MMA provides the copolymer with good electrolyte uptake and reduces the brittleness of the copolymer that results from the use of AN. VAc provides the GPE with strong adhesion between the anode and cathode materials and excellent mechanical stability [45].

Nanofibers/nanowebs produced by electrospinning technique have several remarkable characteristics such as a very big ratio of surface area to volume, pore size within nano range, unique physical characteristics and flexibility for chemical/physical modification and functionalization. It has been shown that the unique properties and multi-functionality of the nanowebs make them very interesting for applications in various areas including biotechnology, textiles and membranes/filters, etc.. Many types of carriers and techniques have been used for the immobilization of β-galactosidase. The most important requirement for a support material is that it should be insoluble in water and have a high capacity to bind with enzyme. β-galactosidase has been immobilized using poly (AN-co-MMA) copolymer nanofibers [46].

2.7 Dielectric Materials

Dielectric materials - or, as they are also called, dielectrics - are such a media that has an ability to store, not conduct, electrical energy [47]. One of the important electrical properties of dielectric materials is permittivity. The real part (eps') of dielectric permittivity is called 'dielectric constant' and its imaginary part (eps") is usually called 'dielectric loss'. For most materials, the dielectric constant is independent of the electric field strenght for fields below a certain critical field, at or above which carrier injection into the material becomes important. The dielectric constant depends strongly on the frequency of the alternating electric field or the rate of the change of the time-varying field. It also depends on the chemical structure and the imperfections (defects) of the material, as well as on other physical parameters including temperature and pressure, etc [48]. The dielectric parameter as a function of frequency is described by the complex permittivity in the form

$$\varepsilon^*(\omega) = \varepsilon'(\omega) - \varepsilon''(\omega) \qquad \textbf{(2.6)}$$

where the real part $\varepsilon'(\omega)$ and imaginary part $\varepsilon''(\omega)$ are the components for the energy storage and energy loss, respectively, in each cycle of the electric field [49].

The investigation of the polarization and transport properties of polymeric samples of mixed character, where chains of a conducting polymer are embedded in a conventional (i.e. dielectric) polymeric matrix, has been subject of a growing interest in recent years [50]. For application of conducting polymers, knowing how these conducting polymer composites will affect the behaviour in an electric field is a long-standing problem and is of great importance. But very little is known about the dielectric properties of conducting polymer associated with the conducting mechanism. Dielectric spectroscopy has been found to be a valuable experimental tool for understanding the phenomenon of charge transport in conducting polymers. Low frequency conductivity and dielectric measurements especially have proven to be valuable in giving additional information on the conducting mechanism that d.c. conductivity measurement alone does not provide [51].

2.8 Electrospinning and Nanofibers

Conventional fiber spinning (like melt, dry and wet spinning) produce fibers with diameter in the range of micrometer. In recent years, electrospinning has gained

much attention as a useful method to prepare fibers in nanometer diameter range. These ultra-fine fibers are classified as nanofibers. The unique combination of high specific surface area, extremely small pore size, flexibility ad superior directional strength makes nanofibers a preferred material form for many applications. Proposed uses of nanofibers include wound dressing, drug delivery, tissue scaffolds, protective clothing, filtration, reinforcement and micro-electronics. For example, carbon fiber hollow nano tubes, smaller than blood cells, have potential to carry drugs in to blood cells. A comparison of hair with nanofibers web is shown in Figure 2.7.

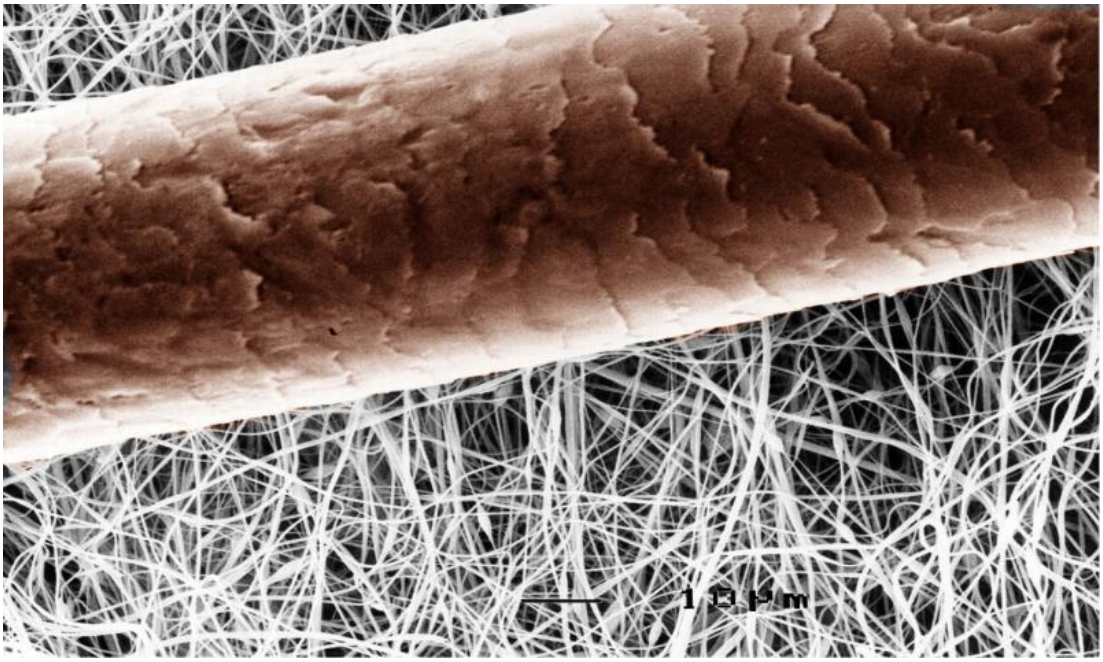

Figure 2.7 : Comparison of hair with nanofibers [52].

In the electrospinning process, a polymer solution held by its surface tension at the end of a capillary tube is subjected to an electric field. Charge is induced on the liquid surface by an electric field. Mutual charge repulsion causes a force directly opposite to the surface tension. As the intensity of the electric field is increased, the hemispherical surface of the solution at the tip of the capillary tube elongates to form a conical shape known as the Taylor cone. When the electric field reaches a critical value at which the repulsive electric force overcomes the surface tension force, a charged jet of the solution is ejected from the tip of the cone. Since this jet is charged, its trajectory can be controlled by an electric field. As the jet travels in air, the solvent evaporates, leaving behind a charged polymer fiber which lays itself randomly on a collecting metal screen.

Thus, continuous fibers are laid to form a nonwoven fabric. Figure 2.8 illustrates the electrospinning setup [53].

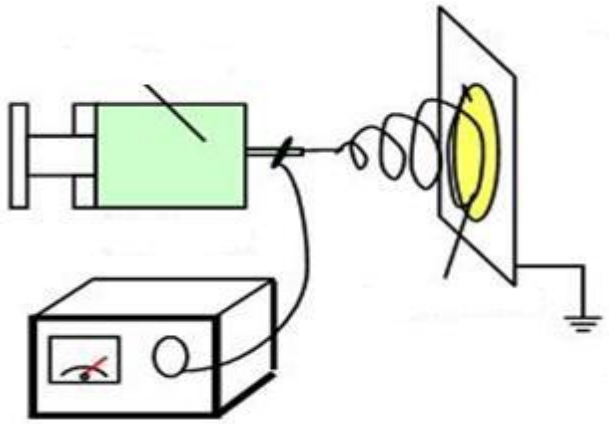

Figure 2.8 : Schematic setup for electrospinning procedure [54].

3. EXPERIMENTAL PART

3.1 Materials

CAN (ammonium cerium (IV) nitrate, $(NH_4)_2[Ce(NO_3)_6]$, Sigma-Aldrich), KPS (potassium peroxodisulfate, $K_2S_2O_8$, Sigma-Aldrich), DBSA (dodecylbenzene sulphonic acid, sodium salt, Sigma-Aldrich), DMF (n,n-dimethylformamide, Merck), EtOH (ethanol, Merck), MMA (methyl methacrylate, $C_5H_8O_2$, Fluka), AN (Acrylonitrile, C_3H_3N, AKSA), Py (Pyrrol, C_4H_5N, Sigma-Aldrich), NMPy (n-methylpyrrol, C_5H_7N, Sigma-Aldrich), NPhPy (n-phenylpyrrol, $C_{10}H_9N$, Sigma-Aldrich). They were used without further purification and all chemicals were analytical grade.

3.2 Characterization

FTIR analysis of P(MMA-co-AN), composite films and nanofibers were carried out with FTIR-ATR reflectance spectrophotometer (Perkin Elmer, Spectrum One, with a Universal ATR attachment with a diamond and ZnSe crystal) (Figure 3.1).

Figure 3.1 : Perkin Elmer, Spectrum One FTIR-ATR Spectrophotometer.

UV-Visible measurements were performed with UV-Visible spectrophotometer (Perkin Elmer, Lambda 45) (Figure 3.2).

Figure 3.2 : Perkin Elmer, Lambda 45 UV-Visible spectrophotometer.

Nuclear Magnetic Resonance measurements were performed with 250 MHz Brucker AC Aspect 3000 using ^{1}H NMR (Figure 3.3).

Figure 3.3 : 250 MHz Brucker AC Aspect 3000 NMR.

Real permittivity, imaginary permittivity and conductivity measurements of composite films were executed with Novocontrol broadband dielectric spectrometer (Alpha-A High Performance Frequency Analyzer, frequency domain 0,001 Hz to 3 GHz) at 25^{o}C (Figure 3.4). Samples were fixed between two copper electrodes with diameters of 20 mm.

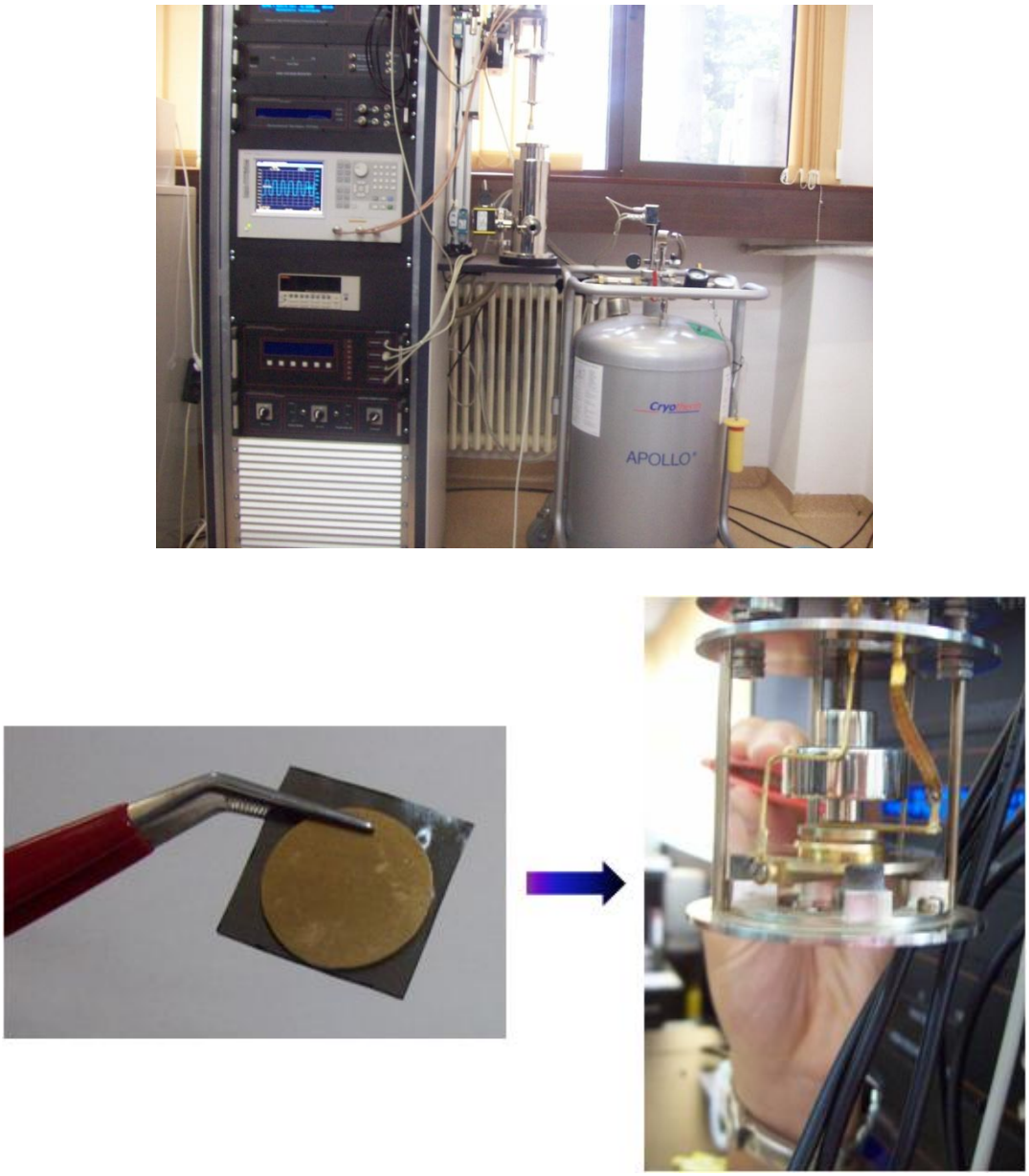

Figure 3.4 : Novocontrol broadband dielectric spectrometer.

Differential Scanning Calorimeter (DSC) measurement was operated with DSC TA Q10 with 3 cycles. Scanning Electron Microscope images of composite films and nanofibers were obtained with LEO SUPRA 35 VP SEM. Nanofiber diameters were measured with Adobe Acrobat 8 Professional.

3.3 PPy/P(MMA-co-AN), PNMPy/P(MMA-co-AN) and PNPhPy/P(MMA-co-AN) Composite Thin Films and Composite Nanofibers

3.3.1 Synthesis of copolymer P(MMA-co-AN)

Poly(methyl methacrylate-co-acrylonitrile) (P(MMA-co-AN)) copolymer was synthesized via the emulsion polymerization with distilled water at 70^{o}C in a glass reactor equipped with a reflux condenser, a mechanical stirrer and a thermometer. Potassium persulfate (KPS) was used as an initiator and dodecylbenzene sulphonic acid, sodium salt (DBSA) was used as an emulsifier. Total moles of monomers was taken as 0.075. Mole values of the substances in the reaction were shown in Table 1. Methyl methacrylate and acrylonitrile were added in the 80 ml deionized water at room temperature. Then, DBSA (surfactant) and KPS (initiator) were added at 40 ^{o}C and at 70 ^{o}C in the solution. The polymerization was continued for 2 h under vigorous stirring. The polymer was isolated by filtration and washed with the hot deionized water for the removal of any impurities such as residual monomers and initiator. The product was then dried in a vacuum oven at 60 ^{o}C under vacuum for 24 h. The copolymer was characterized by FTIR-ATR and DSC.

Table 3.1 : Mole values of the substances in the P(MMA-co-AN) copolymerization.

AN (mole)	**MMA (mole)**	**DBSA (mole)**	**KPS (mole)**	**Water (ml)**
0.06	0.015	0.00230	0.00320	80

3.3.2 Preparation of conductive PPy/P(MMA-co-AN), PNMPy/P(MMA-co-AN), PNPhPy/P(MMA-co-AN) composite films

P(MMA-co-AN) polymer was dissolved at a concentration of 15 wt. % in dimethylformamide (DMF). After complete dissolution Py derivatives (5.5 wt.%, 16 wt.%, 24 wt.%) were added in the solution and mixed for 1 hour at room temperature. Then, CAN (initiator) (50 wt.% of Py derivatives) was added in order to start polymerization. When the initiator was added, solution colour changed immediately due to PPy derivatives formation. Polymerization continued 2 h at 25 ^{o}C. Ethanol twice as much the volume of DMF was added in order to remove excess CAN (initiator) amount. After filtration, the precipitate containing PPy derivatives

was dissolved again in DMF. Then temperature increased to 80 ^{o}C in order to obtain viscous solution. The resulting viscous solution was cast with a 4-sided film aplicator onto a 5-5 cm^2 glass plate. The casted solution was dried under 760 mmHg and 50°C for 24 h. Table 3.2 shows amount of substances using in composite film preparation.

Table 3.2 : Amount of substances using in composite film preparation.

Concentration of Py derivatives (% wt.copolymer)	**P(MMA-co-AN) (g)**	**Py (g)**	**NMPy (g)**	**NPhPy (g)**	**CAN (g)**	**DMF (ml)**
5.5	1.5	0.083	0.083	0.083	0.0415	10
16	1.5	0.24	0.24	0.24	0.12	10
24	1.5	0.36	0.36	0.36	0.18	10

3.3.3 Preparation of conductive PPy/P(MMA-co-AN), PNMPy/P(MMA-co-AN), PNPhPy/P(MMA-co-AN) composite nanofibers

The solution in section 3.3.2 was also used for preparation of conductive composite nanofibers. The solution of PPy derivatives/P(MMA-co-AN) was loaded into a syringe and a positive electrode was clipped onto the syringe needle, having an outer diameter of 0.9 mm. The feeding rate of the polymer solution was controlled by electrospinnig apparatus consisted of a syringe pump and the solutions were electrospun horizontally onto the collector that was covered with aluminum foil. The electrospinning conditions are given below:

Solution Concentration: 15 wt.%

Applied Voltage: 20 kV

Tip to Collector Distance: 15 cm

Feed Rate: 0.5 ml/h

4. RESULTS AND DISCUSSION

4.1 Characterization of P(MMA-co-AN)

4.1.1 FTIR-ATR analysis

Figure 4.1 presents the FTIR-ATR spectra of monomers, MMA, AN and their copolymer P(MMA-co-AN) (monomer feed ratio, AN:MMA 80:20). The characterwastic absorption peaks of MMA were at 1639 cm^{-1} for the bond C=C, at 1723 cm^{-1} for the stretching bond of C=O and at 1100–1200 cm^{-1} the peaks of the stretching vibration of the C-O-C. The monomer AN showed its characterwastic absorption at 2232 cm^{-1} which correspond to C≡N group. The characterwastic peaks of the monomers shifted to 1739 cm^{-1} for C=O, and 2242 cm^{-1} for C≡N and also the absorption peak at 1639 cm^{-1} for C=C lost in FTIR spectrum of the copolymer P(MMA-co-AN). This indicated the copolymer was obtained by the way of the breaking C=C double bonds and maintained the main characteristics of the monomers [55,56].

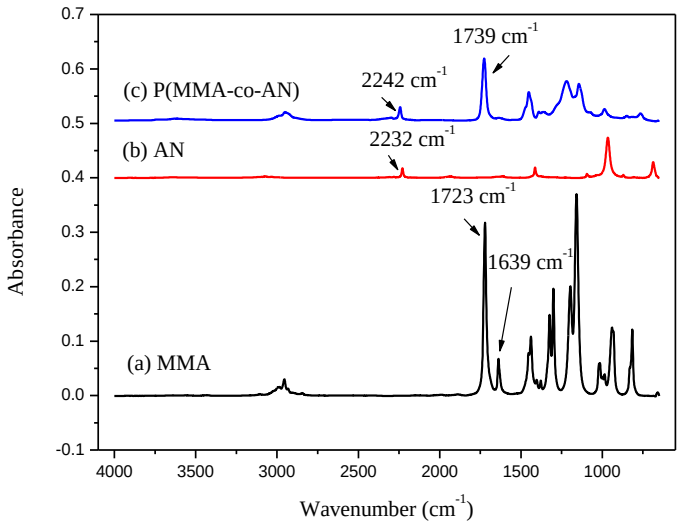

Figure 4.1 : FTIR-ATR spectra of monomers (a) MMA, (b) AN and copolymer (c) P(MMA-co-AN).

4.1.2 DSC analysis

The DSC thermogram of P(MMA-co-AN) is shown in Fig. 4.2. The glass transition temperature (Tg) of dried copolymer product was 98^{o}C, much lower than that of pure PMMA (113^{o}C), much higher than that of pure PAN (about 90^{o}C) [57,58]. This confirmed that the copolymer was formed by the copolymerization among two monomers rather than the co-mixture of PAN and PMMA.

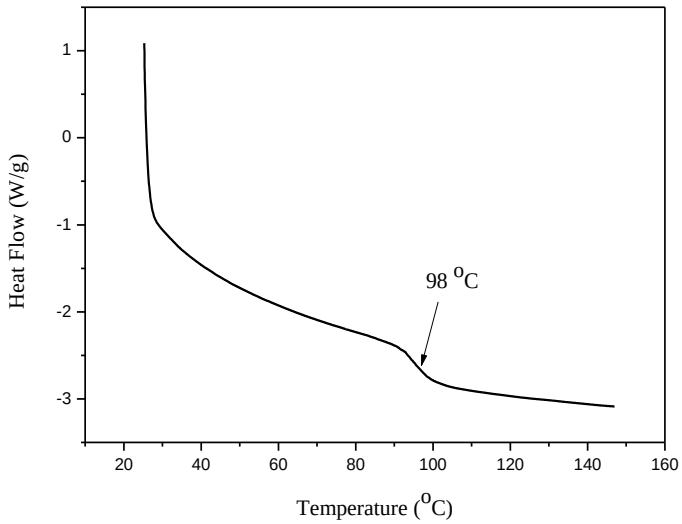

Figure 4.2 : DSC curve of P(MMA-co-AN).

4.1.3 NMR analysis

^{1}H NMR result was used to calculate the copolymer composition over the entire composition range used. Figure 4.3 represents the ^{1}H NMR of 65%AN:35%MMA copolymer (mole:mole). The peak at 2.06-2.18 ppm was assigned to methylene (CH_2) protons in the MMA and AN units. The peaks appearing in the range of 1.01-1.30 ppm correspond to α-methyl (CH_3) protons in the MMA unit. The methoxy protons linked to the adjacent carbonyl group in the MMA unit was found at 3.63-3.74 ppm. The methine proton peak in the AN unit appeared at 3.15-3.2 ppm [59]. The composition of the copolymer could be determined from the relative intensities of the peaks of the α-methyl protons in MMA unit and the methylene protons in ^{1}H NMR spectrum (Figure 4.3).

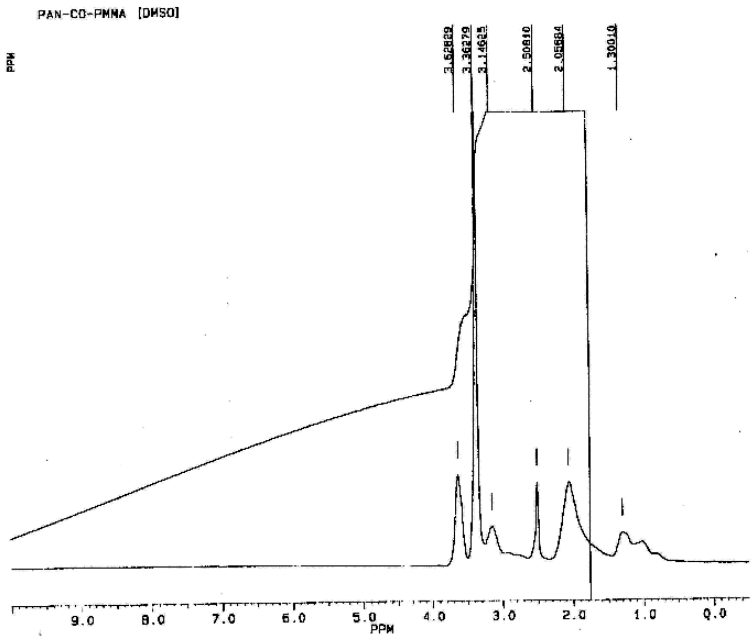

Figure 4.3 : ^{1}H NMR spectroscopy of P(MMA-co-AN) in DMSO-d_6 solvent.

Mole fraction of AN unit:

$1-(1/3)A_{1.01\text{-}1.30\ ppm}/(1/2)A_{2.06\text{-}2.18\ ppm} = 0.6518$

Mole fraction of MMA unit:

$1-0.6518 = 0.3482$

The mole fraction of AN in the P(MMA-co-AN) copolymer was determined to be 0.65 from the ^{1}H NMR spectrum shown in Figure 4.3. The copolymer with a higher AN content could not be synthesized, which is caused by the comparatively poor reactivity of AN for copolymerization [60]. The composition of the copolymer synthesized is listed in Table 4.1.

Table 4.1 : Molar composition of PMMA and PAN in P(MMA-co-AN).

	Composition of AN (mole %)	
Polymer	**In feed**	**In copolymer**
AN65	80	65

4.2 Characterization of PPy/P(MMA-co-AN), PNMPy/P(MMA-co-AN) and PNPhPy/P(MMA-co-AN) Composite Thin Films

4.2.1 FTIR-ATR analysis

Figure 4.4 shows infrared spectra of *N*,*N*-dimethylformamide and P(MMA-co-AN) film prepared from *N*,*N*-dimethylformamide. In the P(MMA-co-AN) film spectrum, the following characteristic features appeared due to the copolymer structure, the stretching peak of C=O in carbonyl groups at 1725.53 cm^{-1}; the peaks of the bend vibration of $-CH_2$ and $-CH_3$ groups at 1451.93 and 1388.55 cm^{-1}, the peaks of the stretching vibration of the C-O-C and C-H groups at 1100–1200 cm^{-1} and 3000–2840 cm^{-1}, the peak of nitrile group CN at 2242.54 cm^{-1} . The main characteristic IR band of DMF C=O stretching at 1661.01 cm^{-1} shifted to 1667.27 cm^{-1}. This indicates interaction of DMF amide groups with the methyl groups and nitrile groups of P(MMA-co-AN). This interaction decreases stiffness and hardness of PPy/P(MMA-co-AN) composite films, increases its segmental motion. Such segmental motion produces voids or free volume which enables the easy flow of ions through the material when there is an applied electric field [61,62,63,43].

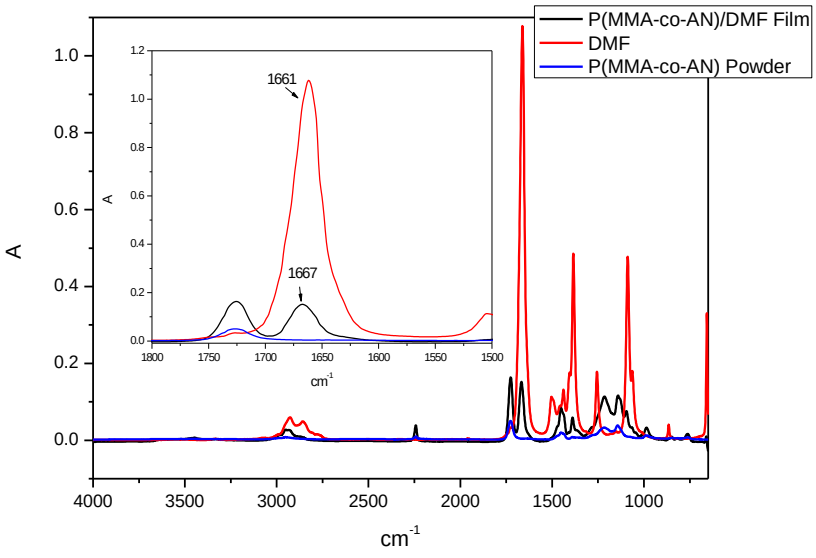

Figure 4.4 : FTIR-ATR results of pure DMF (a) and P(MMA-co-AN) composite film by using DMF as solvent (b).

Pyrrole and its derivatives showed similar infrared spectras. Characteristic peaks of the conducting polymer component became discernible at a mass loading of 24%.

Figure 4.5, Figure 4.6 and Figure 4.7 represents FTIR spectroscopic analysis of P(MMA-co-AN) and PPy derivatives/P(MMA-co-AN) composite thin films at different mass loading. The NH stretching band of pyrrole ring appeared at 3218 cm^{-1}. The weak band at 2950 cm^{-1} was due to C–H stretching. The peak at 1312 cm^{-1} showed C–H in-plane deformation of the pyrrole [64,65,66]. According to literature $–NO_3$ group of Cerium (III) shows characteristic band at 1319 cm^{-1} [67]. There was a significant absorbance increase in the peak of 1312 cm^{-1} at 24% mass loading of Py derivatives. There might be two explanations for this obvious increase, increase in PPy derivatives amount in the composite films or $–NO_3$ group of Cerium (III) in the complex structure consists of matrix P(MMA-co-AN), solvent (DMF) and PPy derivatives. Conjugated C–N ring stretching peak of the pyrrole at 1436 cm^{-1} showed increase and shifting upon increasing the conducting polymer content in the P(MMA-co-AN) matrix (Figure 4.5). As the PPy, PNMPy and PNPhPy increased in the composite films C=O stretching peak of DMF appeared as broader at lower wavenumber around 1649 cm^{-1}. This might be due to ionic interaction between carbonyl group of DMF (C=O) having a partially negative charge and NH group of PPy having a partially positive charge. According to information from the literature C=C ring stretching of pyrrole occurs at 1626 cm^{-1} [67]. Increasing of C=C bonds with PPy, PNMPy and PNPhPy loading may cause also broaden of carbonyl peak at 1649 cm^{-1}. The other spectra also show the characteristic polypyrrole absorption at 1600–650 cm^{-1}. The band at 1036 cm^{-1} may correspond to =C-H band in plane vibration. The IR peak observed at 819 cm^{-1} may be assigned to the =C–H out of plane vibration indicating polymerization of pyrrole. Bands observed at 735 and 674 cm^{-1} showed the presence of polymerized pyrrole [68].

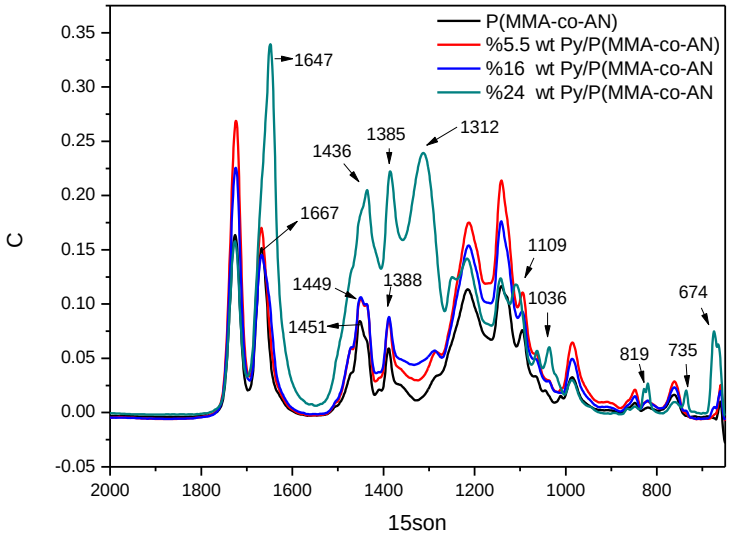

Figure 4.5 : FTIR-ATR results of PPy/P(MMA-co-AN) composite films at different Py loading.

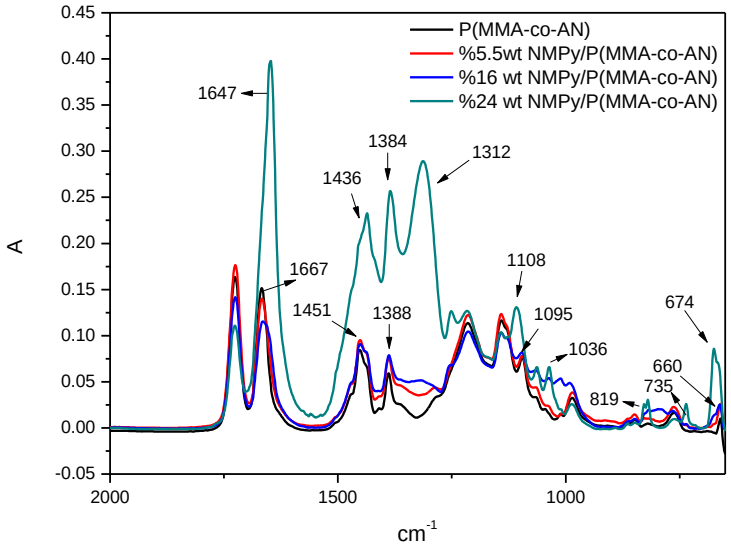

Figure 4.6 : FTIR-ATR results of PNMPy/P(MMA-co-AN) composite films at different NMPy loading.

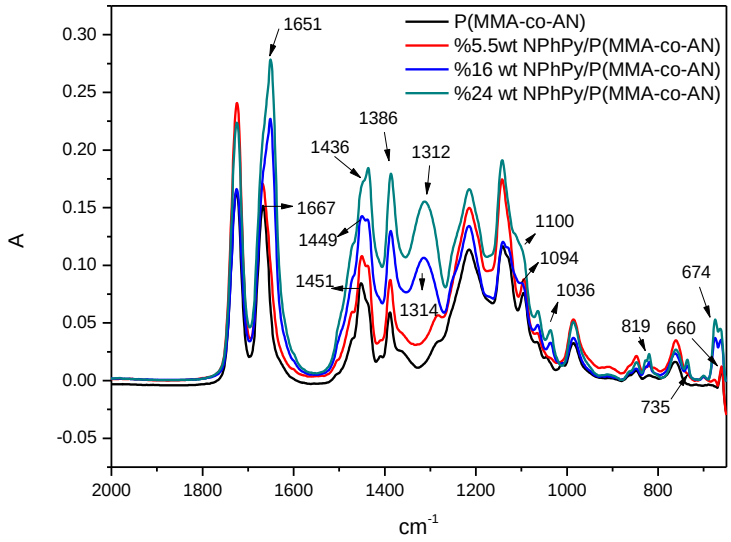

Figure 4.7 : FTIR-ATR results of PNPhPy/P(MMA-co-AN) composite films at different NPhPy loading.

Figure 4.8 and Figure 4.9 shows increasing in the absorbance of the main characteristic peaks of PPy derivatives.

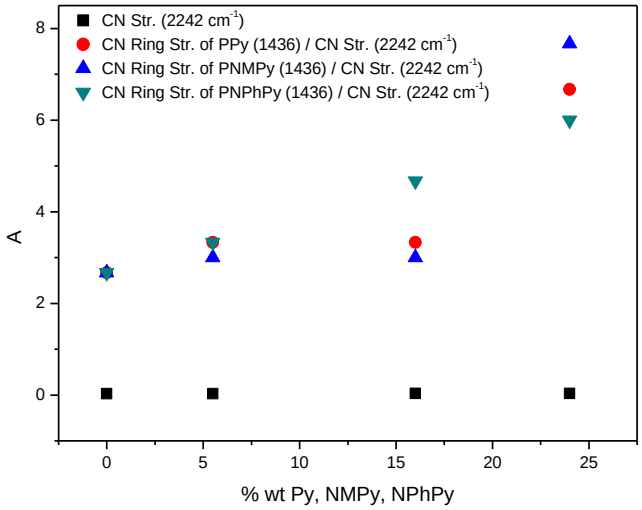

Figure 4.8 : Linear relationship between absorbance ratio of the main characteristic peaks and % mass loading of PPy derivatives.

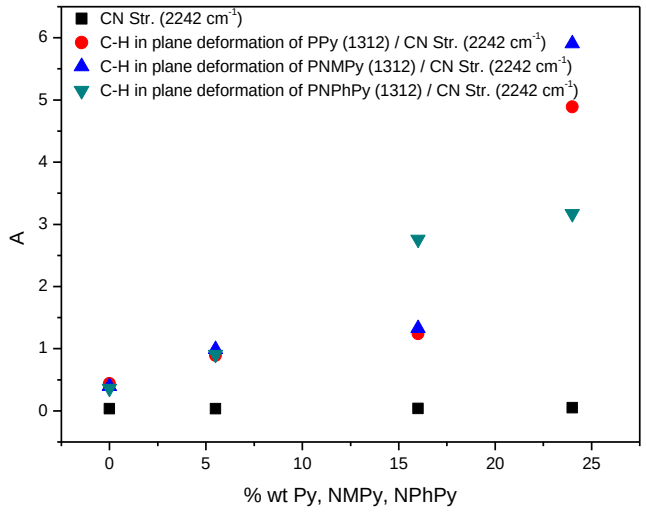

Figure 4.9 : Linear relationship between absorbance ratio of the main characteristic peaks and % mass loading of PPy derivatives.

4.2.2 UV-Visible analysis

The UV–vis spectra of the PPy/P(MMA-co-AN), PNMPy/P(MMA-co-AN) and PNPhPy/P(MMA-co-AN) are shown in Figure 4.10, Figure 4.11 and Figure 4.12. The UV–vis spectrum in DMF (*n*,*n*-dimethylformamide) solution showed a band near the ultraviolet region (315 nm) and a weak band in visible region (462 nm) and a broad band at around 640 nm. The band at 315 nm was related to the interband $\pi \rightarrow \pi^*$ transitions of the aromatic form of neutral polypyrrole. The band at 462 nm, on the other hand, was believed to be due to a slight residual doping. The band at 640 is assigned to the bipolaron state of PPy [69,70].

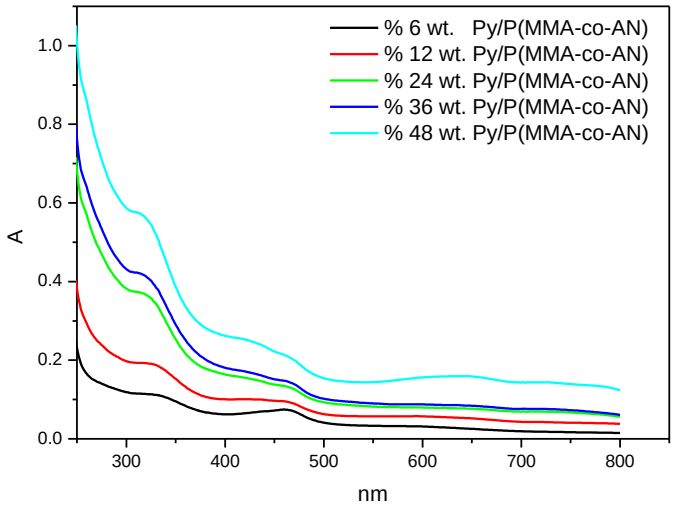

Figure 4.10 : UV-Visible spectras of PPy/P(MMA-co-AN) Composite Thin Films.

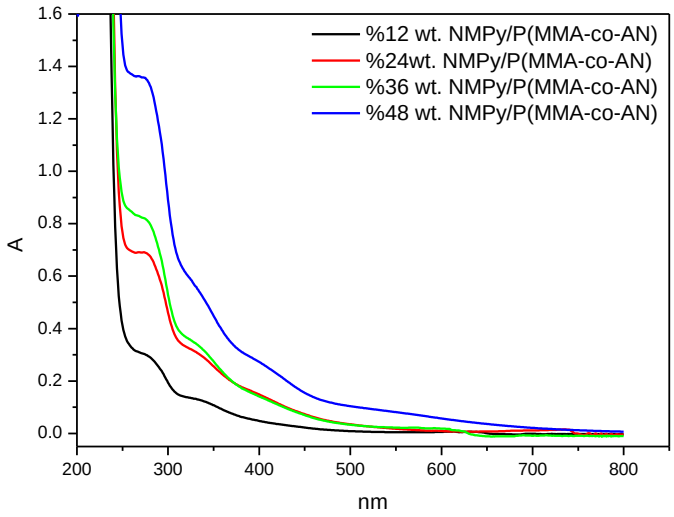

Figure 4.11 : UV-Visible spectras of PNMPy/P(MMA-co-AN) Composite Thin Films.

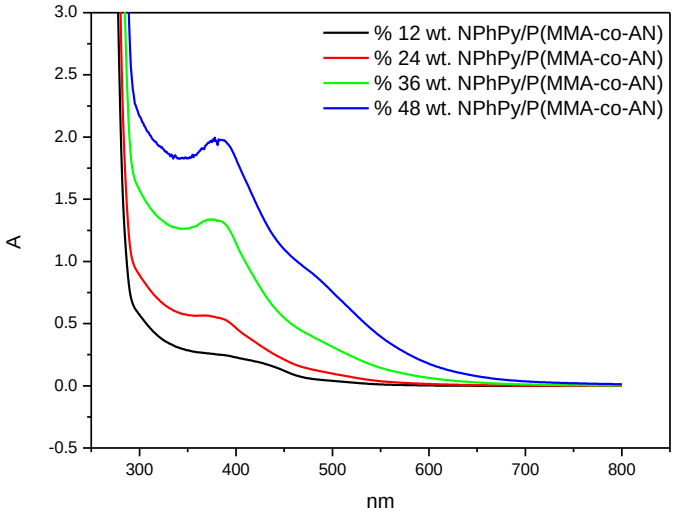

Figure 4.12 : UV-Visible spectras of PNPhPy/P(MMA-co-AN) Composite Thin Films.

4.2.3 NMR analysis

The ^{1}H NMR spectra of each sample was recorded in DMSO-d_6. The ^{1}H NMR spectra of composite films are shown in Figure 4.13. The peaks at 7.0-8.5 ppm in the spectra of polypyrrole derivatives were assigned to the aromatic protons on pyrrole ring [71]. PNPhPy has broader more visible peaks with higher integral value in this range. Such broadening in the NMR spectra of conducting polymers is related to increase in conductivity [72]. According to this statement the order of conductivity of composite films is as follows: PPy/P(MMA-co-AN)<PNPhPy/P(MMA-co-AN). This result is parallel with a.c. conductivity measurements. –NH protons of pyrrole groups at 3.8-3.4 ppm could not be identified, as the DMSO-d_6 protons give peaks in the same region [73].

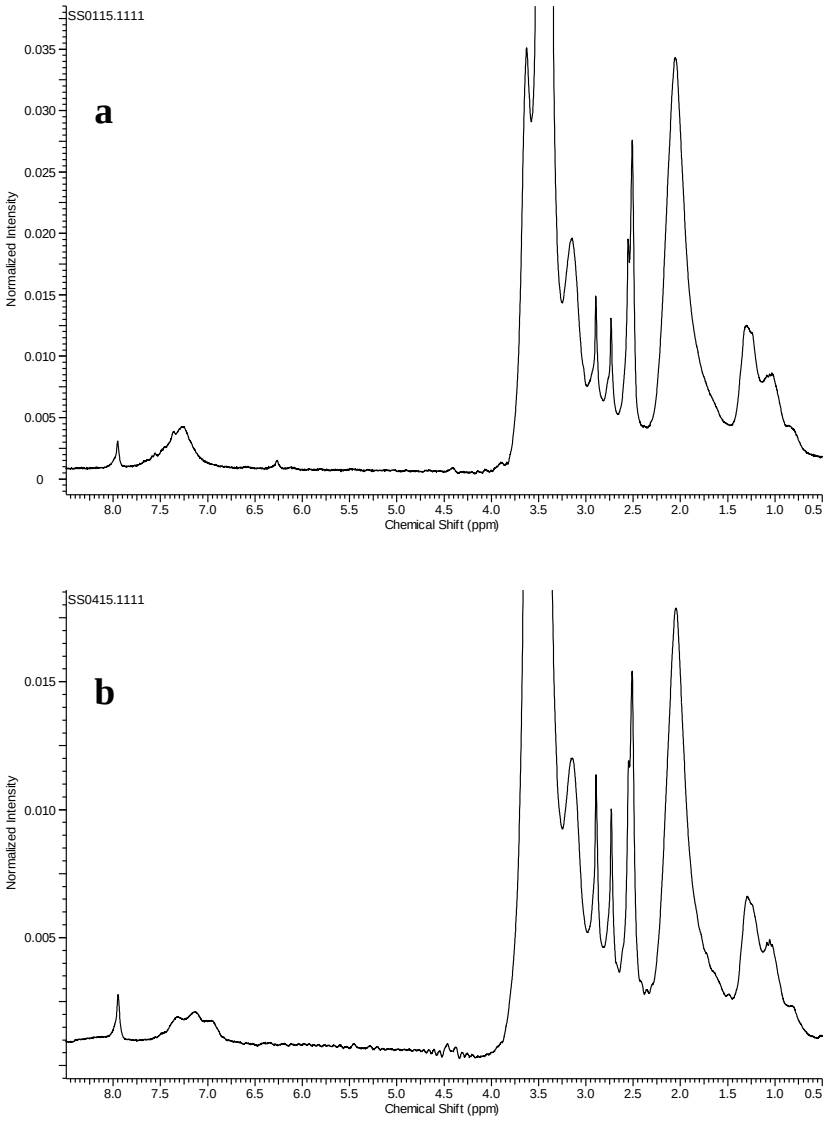

Figure 4.13 : NMR Analysis of a) PNPhPy/P(MMA-co-AN); b) PPy/P(MMA-co-AN) Composite Thin Films.

4.2.4 Dielectric spectroscopic analysis

Dielectric properties of composites were evaluated on the basis of dielectric constant, dielectric loss, electric modulus, and AC conductivity and their variation with frequency. Dielectric measurements were carried out at room temperature (25 ^{o}C). Figure 4.14, Figure 4.15, Figure 4.16 shows the frequency dependence of dielectric constant (ε') of the composite thin films containing various amount of PPy derivatives. The dielectric constant of composite thin films decreased gradually with increasing frequency. This may be attributed to the tendency of dipoles in polymeric samples to orient themselves in the direction of the applied field. However at the high frequency range ($1x10^4$ Hz to $1x10^7$ Hz), the decreasing trend seemed not too

sharp as compared for lower frequency region. This trend was observed for all graphs for different concentration of PPy derivatives. It could be explained by dipoles orientation, which difficult to rotate at high frequency range. On the other hand, the high value of (ε') at low frequency might be due to the the space charge polarization, the mobility of charge carrier to the interface between the conjugated polymer and the insulating matrix, in addition to dipolar polarization [74, 75].

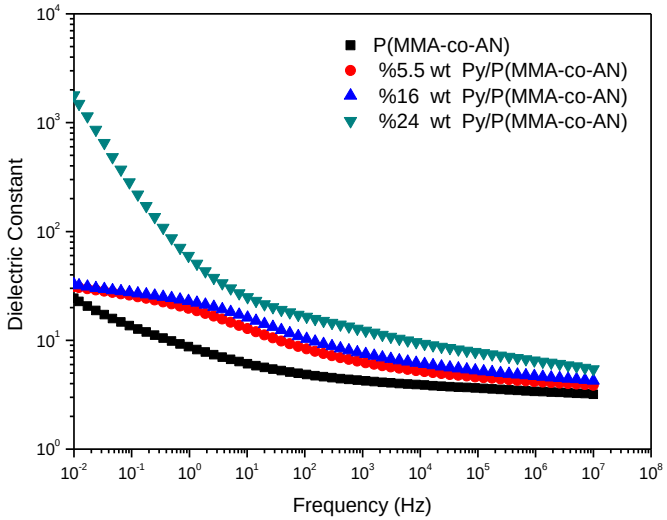

Figure 4.14 : The dielectric constants of PPy/P(MMA-co-AN) composite thin films at 25°C for different Py loading.

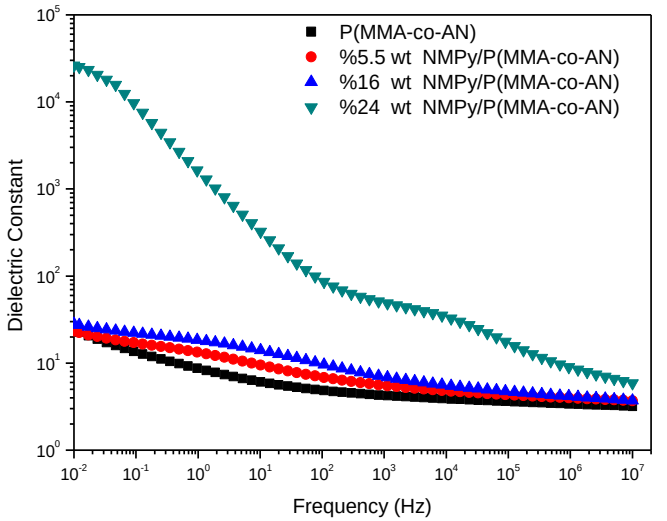

Figure 4.15 : The dielectric constants of PNMPy/P(MMA-co-AN) composite thin films at 25°C for different NMPy loading.

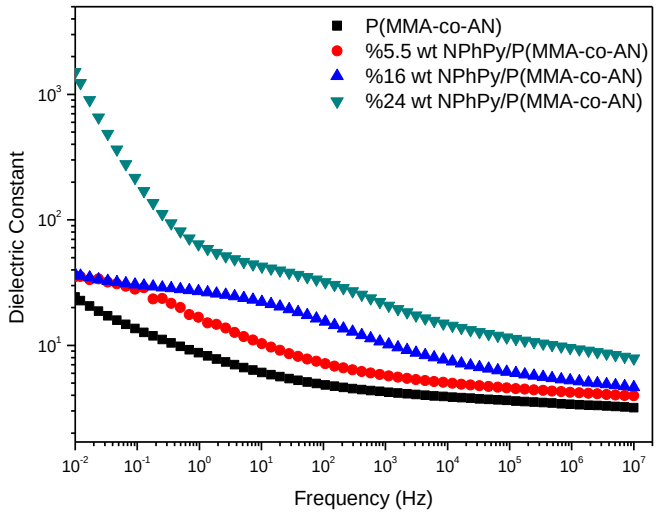

Figure 4.16 : The dielectric constants of PNPhPy/P(MMA-co-AN) composite thin films at 25^{o}C for different NPhPy loading.

As it is seen in Figure 4.14, Figure 4.15, Figure 4.16 the (ε') value did not show any remarkable change from %5.5 to %16 mass loading of Py derivatives. An increase of the dielectric constant observed for Py derivatives especially at %24 wt. and at lower frequencies. At the same initially added Py, NMPy and NPhPy concentrations (%24 wt.), the dielectric constant values were obtained as 283.2, 9702.8, and 216.5, respectively, at 10^{-1} Hz. The P(MMA-co-AN) film's dielectric constant was measured 13.6 at 10^{-1} Hz. In PPy, one dimensional chain of identical monomer units has π electrons but upon polymerization the spatial extent of these electrons is influenced by significant overlap and the electrons become delocalized over the length of the polymer chain in the form of bands analogous to that of a semiconductor and the distortion of the polymer chain around the injected charge carriers leads to formation of polarons [76]. In PNMPy steric interactions between the H's on the N-methyl groups and the β-hydrogens on the adjacent rings force a twisted chain conformation of the polymer backbone. Difference in polymer chain and regular distribution of PNMPy in polymer matrix may cause higher dielectric constant and dielectric loss compared to PPy and PNPhPy.

The sharp increase of dielectric loss (ε'') is the characteristics of charge carrier systems (Figure 4.17, Figure 4.18, Figure 4.19). The localized charge carriers under an applied alternating electric field can hop to neighboring localized sites like the

reciprocating motion of a jumping dipole or can jump to neighboring sites, which form a continuous connected network allowing the charges to travel through the entire physical dimensions of the polymer sample and causing the electric conduction. During the motion of charge carriers, the applied electric field will be a subject of decay. Such relaxation of electric field is termed electric field relaxation and the relaxation of the charge system is termed conductivity relaxation [77]. The oscillatory behavior of ε" may be due to some relaxation processes which usually occur in heterogeneous system. The relaxation peaks appeared clearly for all PPy derivative concentrations. The increasing of PPy derivative concentration increased the height of the peak and its broadness. This indicates the enhancement of conductivity in the composite, enhancement of losses as result of PPy derivative addition [74].

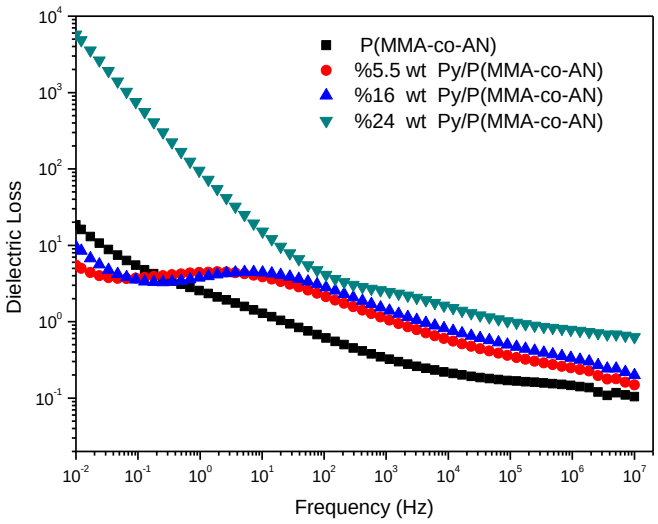

Figure 4.17 : The dielectric losses of PPy/P(MMA-co-AN) composite thin films at 25^{o}C for different Py loading.

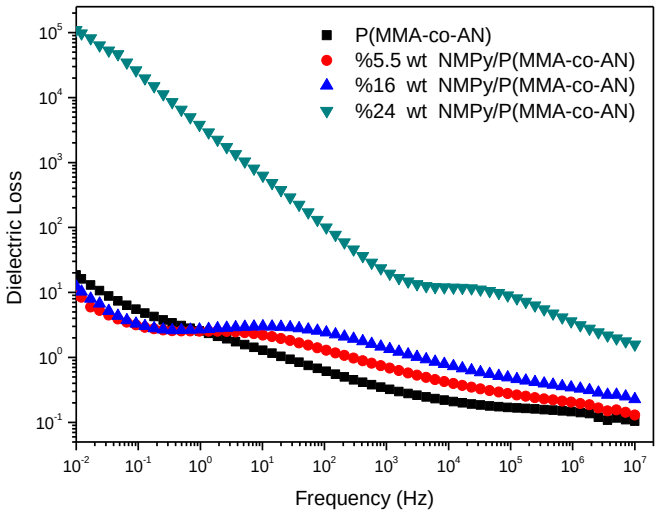

Figure 4.18 : The dielectric losses of PNMPy/P(MMA-co-AN) composite thin films at 25^{o}C for different NMPy loading.

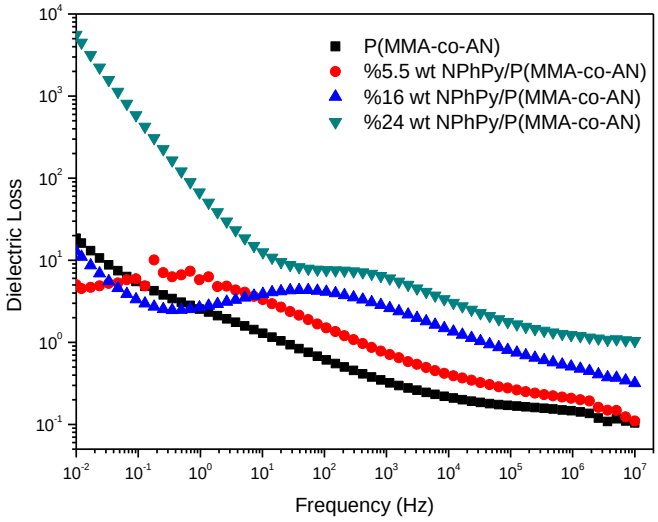

Figure 4.19 : The dielectric losses of PNPhPy/P(MMA-co-AN) composite thin films at 25^{o}C for different NPhPy loading.

The frequency dependent electrical conductivities (AC conductivity) of composite thin films carried out at room temperature (25 ^{o}C) are shown in Figure 4.20, Figure 4.21, Figure 4.22. Linear correlation was observed between the absorbance values of CH in plane deformation of pyrrole peaks attained from FTIR-ATR spectrums and conductivities from dielectric spectrometers. In order to show correlation, the absorbance and conductivity values of composite thin films were plotted as a function of the initially added pyrrole derivative concentrations as an inset images.

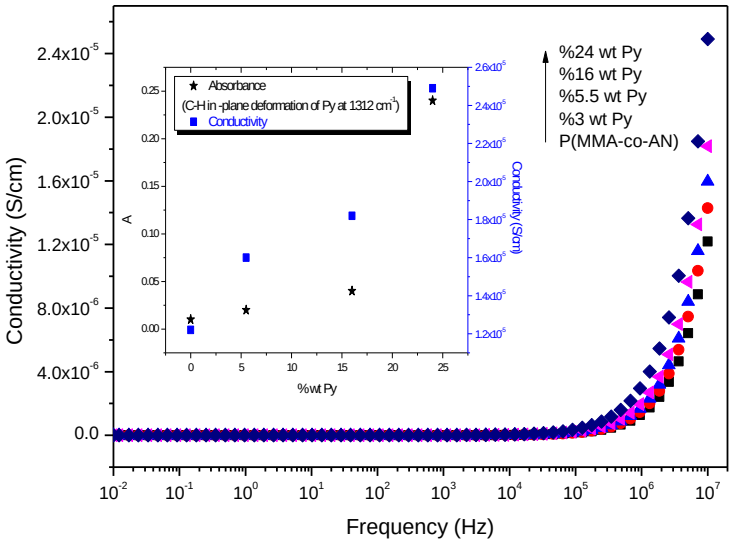

Figure 4.20 : Frequency dependence of composite thin films a.c. conductivity at different Py concentrations.

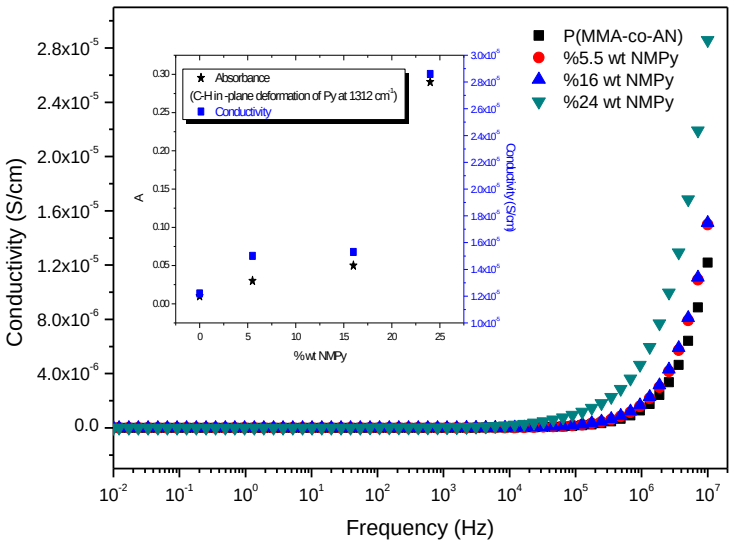

Figure 4.21 : Frequency dependence of composite thin films a.c. conductivity at different NMPy concentrations.

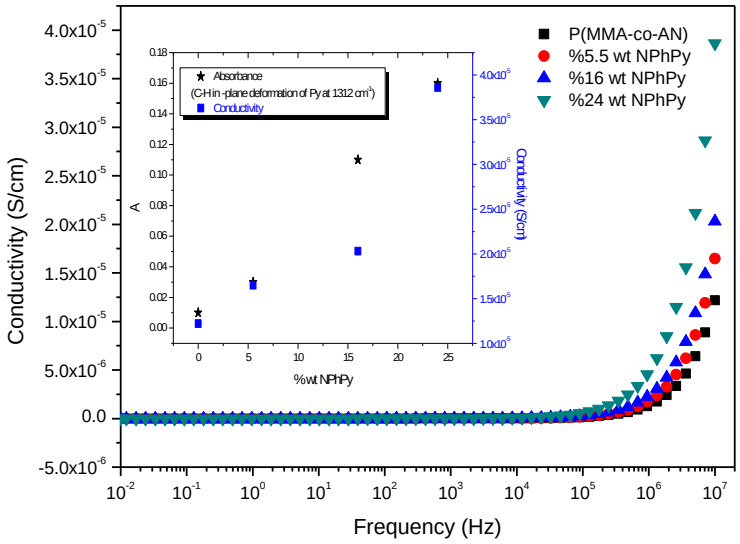

Figure 4.22 : Frequency dependence of composite thin films a.c. conductivity at different NPhPy concentrations.

At lower frequencies between 10^{-2} and 10^{5} Hz, in all composite thin films we observed that conductivity became almost independent of frequency. All the composite films showed similar behavior up to 10^{5} Hz and there was not much variation in the conductivity with frequency during this range. This may be due to random diffusion of the charge carriers, via activated hoping, which is known to give rise to a frequency independent conductivity [78]. At higher frequencies (10^{5}–10^{7} Hz), there was an obvious increase in the composite film conductivity with increasing frequency due to formation of excess charge carriers (polaron and bipolaron) at higher frequencies [68]. This behavior is common for polymeric and semiconductor samples [79,80].

In our measurements, we determined the conductivity of P(MMA-co-AN) film without pyrrole derivatives as 1.3×10^{-7} S/cm at 10^{5} Hz. Also %24 wt. concentration of PPy, PNMPy and PNPhPy based composite films' conductivities at 10^{5} Hz are 3.5×10^{-7} S/cm, 9.5×10^{-7} S/cm and 7.3×10^{-7} S/cm, respectively. So we can conclude that our films are in the semi conductive range. At higher frequencies than 10^{5} Hz, the composite films have shown typical semi conductive character.

Figure 4.23 shows the conductivity comparison for different pyrrole derivatives at 10^{7} Hz for 25 ^{o}C. There is an obvious increase in the conductivity of PNPhPy/

P(MMA-co-AN) composite films with increasing n-phenyl pyrrole concentrations compared to the other composite films. For a selected concentration of %24 wt. of composite films at 10^7 Hz, the conductivity was found to be in the following order: PPy/P(MMA-co-AN)<PNMPy/P(MMA-co-AN)<PNPhPy/P(MMA-co-AN).
Substitution groups of PPy, methyl and phenyl ring, obtain more regular conjugation compared to pyrrole [43].

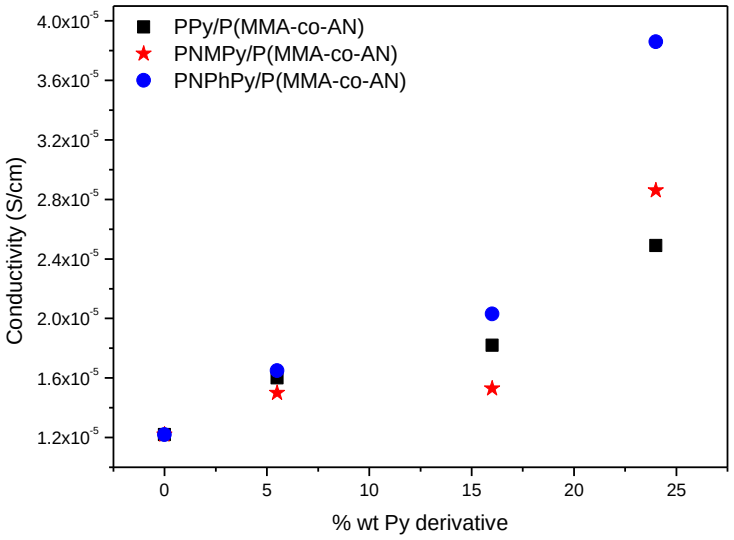

Figure 4.23 : Conductivity comparison with different pyrrole derivatives amount at 10^7 Hz and 25 ^oC.

4.2.5 Morphologic analysis

The typical scanning electron microscope (SEM) images of the PPy derivatives/P(MMA-co-AN) composite films are shown in Figure 4.24, Figure 4.25. It is interesting to find that there are many pores dispersed in the composite films. Moreover, the pores density increases with the increase of PPy derivative content in the films (Figure 4.24, Figure 4.25). It should be noted that the composite films were made by casting process, and a phase separation must occur more or less during the process of solvent volatilization. As a result, CAN (ammonium cerium (IV) nitrate) did not disperse in Py derivative/P(MMA-co-AN) very uniformly. After the removal of the formed organic salt by ethanol, pores were left in the films because PPy derivative and P(MMA-co-AN) are insoluble in ethanol [81,82,83].

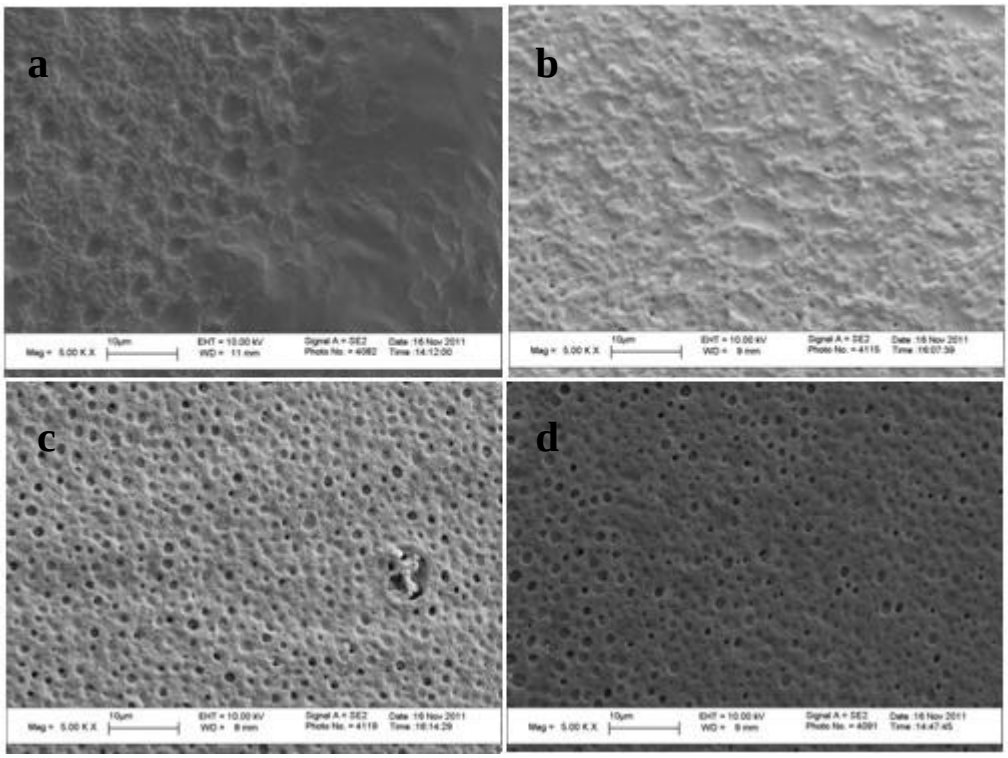

Figure 4.24 : SEM images of the PPy derivatives/P(MMA-co-AN) composite thin films with various weight contents (wt.%) of Py derivatives. a) P(MMA-co-AN); b) 5.5 % Py/P(MMA-co-AN); c) 16 % Py/P(MMA-co-AN); d) 5.5 % NMPy/P(MMA-co-AN).

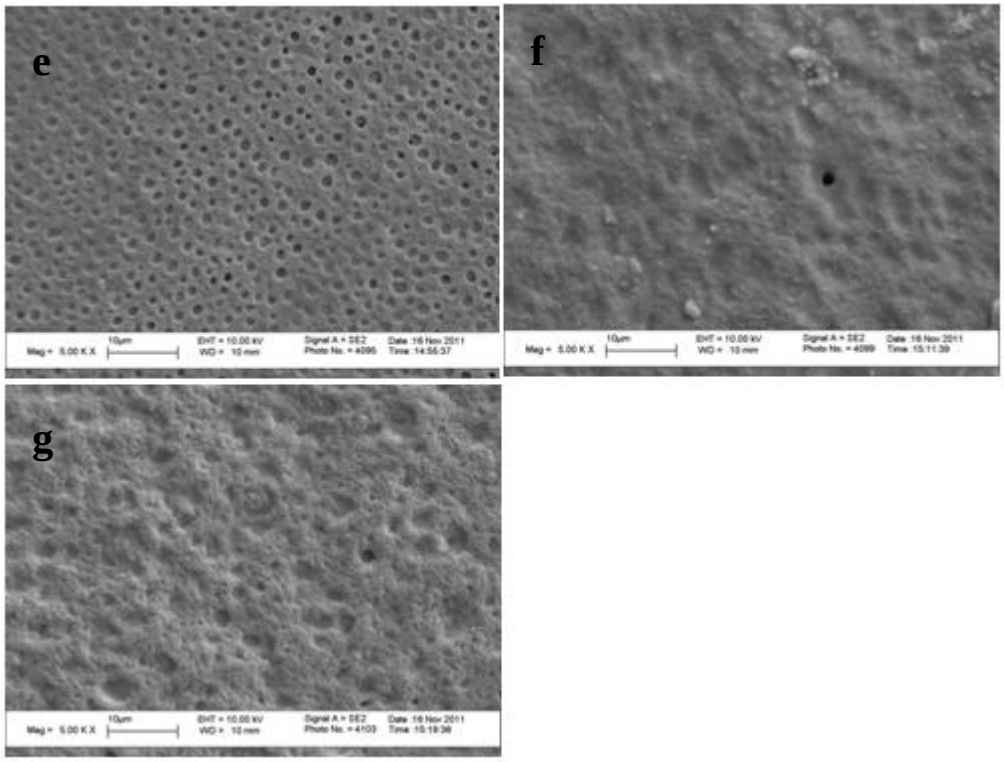

Figure 4.25 : SEM images of the PPy derivatives/P(MMA-co-AN) composite thin films with various weight contents (wt.%) of Py derivatives. e) 16 % NMPy/P(MMA-co-AN); f) 5.5 % NPhPy/P(MMA-co-AN); g) 16 % NPhPy/P(MMA-co-AN).

4.3 Characterization of PPy/P(MMA-co-AN), PNMPy/P(MMA-co-AN) and PNPhPy/P(MMA-co-AN) Composite Nanofibers

4.3.1 FTIR-ATR analysis

Figure 4.26 shows the FT-ATR spectra of the composite nanofibers. The characteristic C=N stretching and in plane =C–H stretching of PPy derivatives were located at 1448 and 1310 cm^{-1} [84,85].

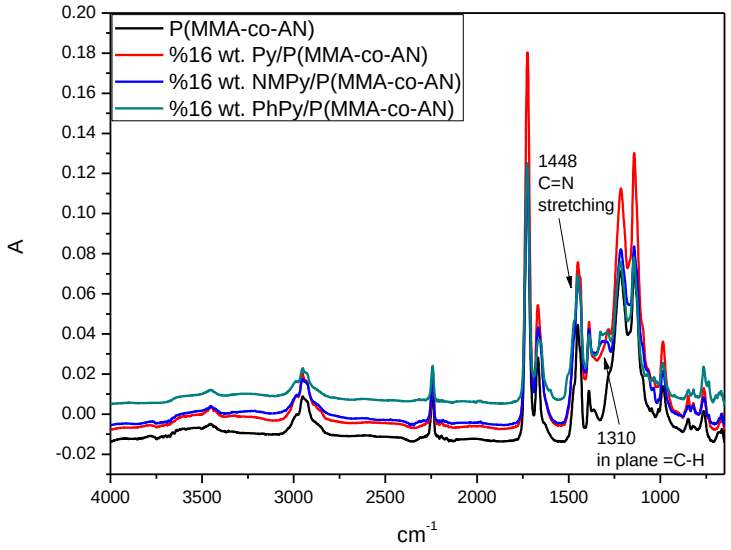

Figure 4.26 : FTIR-ATR results of PPy/P(MMA-co-AN), PNMPy/P(MMA-co-AN), PNPhPy/P(MMA-co-AN) composite nanofibers at 16 % wt. Py derivatives loading.

4.3.2 UV-Visible analysis

For the inclusion of PPy derivatives, further support was obtained from the ultraviolet-visible (UV-Vis) spectrums of PPy/P(MMA-co-AN), PNMPy/P(MMA-co-AN) and PNPhPy/P(MMA-co-AN) composite nanofibers at %24 mass loading. DMF (*n*,*n*-dimethylformamide) was used as solvent. Three bands were slightly occured at 416, 340 and 560 nm for PPy derivatives. These represent the $\pi \rightarrow \pi^*$ and bipolaron excitations [85,86,87].

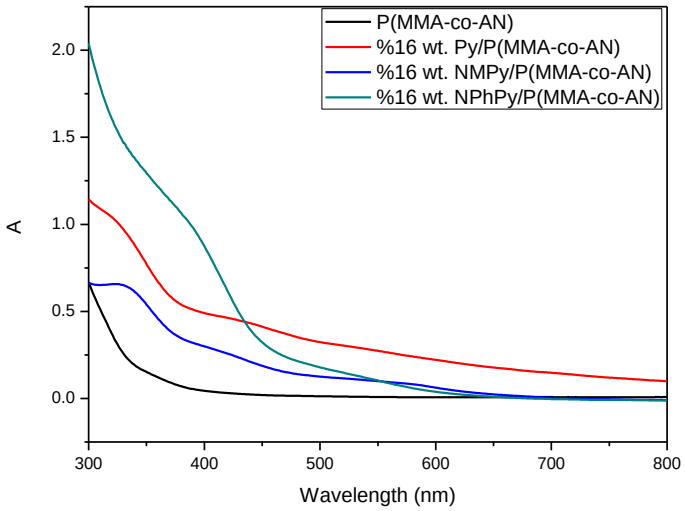

Figure 4.27 : UV-Visible spectras of PPy/P(MMA-co-AN), PNMPy/P(MMA-co-AN) and PNPhPy/P(MMA-co-AN) composite nanofibers at % 16 wt. Py derivatives loading.

4.3.3 Morphologic analysis

The morphologies of nanofibers without PPy derivatives are presented in Figures 4.28 and 4.29. According to the scanning electron microscope (SEM) images, the diameter of the P(MMA-co-AN) nanofibers are dependent on initially added copolymer concentrations in the reaction mixture (Figures 4.28, 4.29). When the weight percentage of the initially added P(MMA-co-AN) concentration varies from 15 % to 20 %, the average diameters of the nanofibers are increased from 285 to 1516 nm (Figure 4.30).

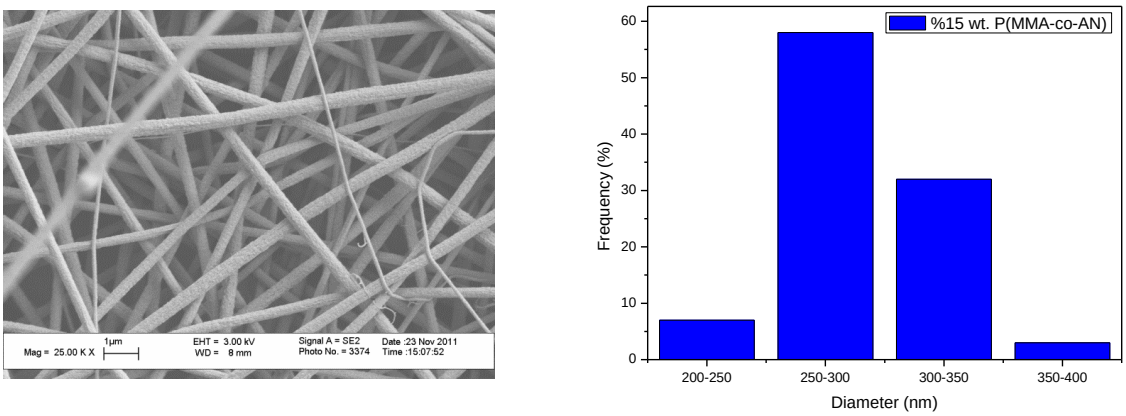

Figure 4.28 : SEM images of P(MMA-co-AN) nanofibers with 15 wt % solution.

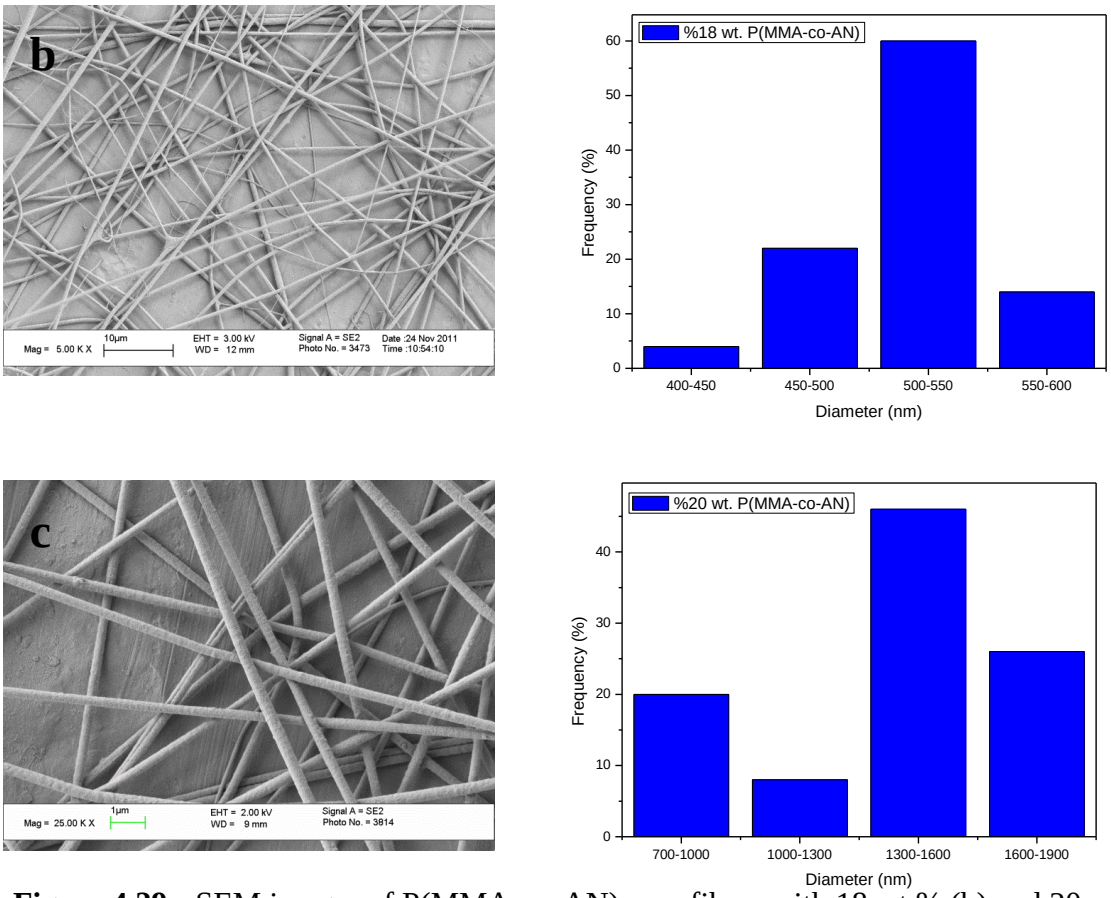

Figure 4.29 : SEM images of P(MMA-co-AN) nanofibers with 18 wt % (b) and 20 wt % (c) solution.

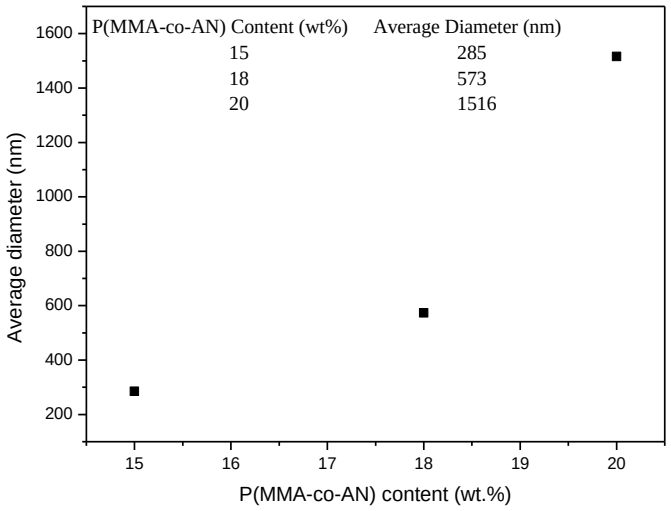

Figure 4.30 : Average diameters of nanofibers electrospun at different P(MMA-co-AN) weight concentration.

Figure 4.31 shows SEM images of electrospun P(MMA-co-AN)/PPy nanofibers with different PPy contents (5.5, 16, and 24 wt%). It was seen that all nanofibers have

regular and straight fibrous morphology. Uniform fibers with average diameter of 346 nm could be electrospun successfully from 15 wt. % P(MMA-co-AN)/DMF solution for three different PPy contents.

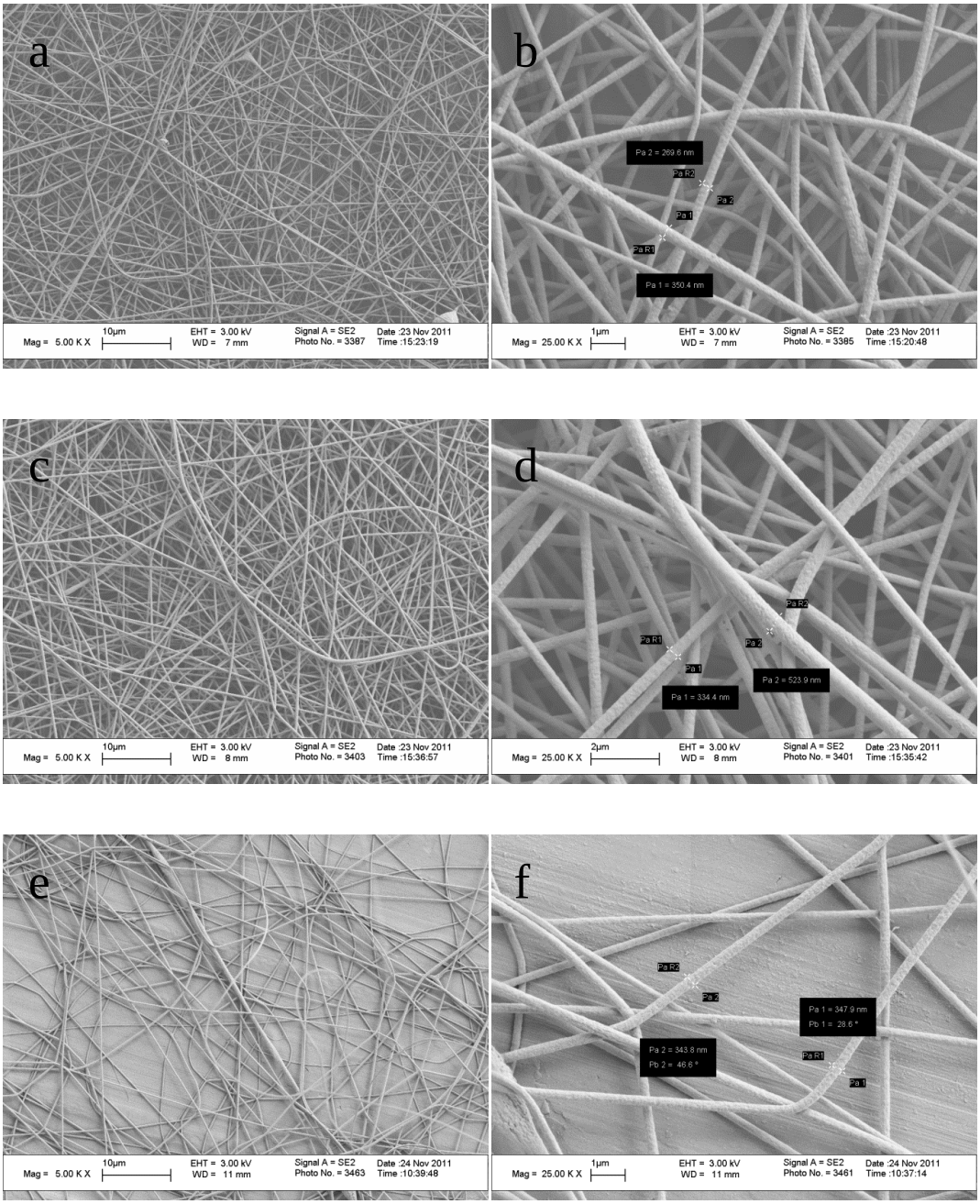

Figure 4.31 : Scanning electron micrographs of electrospun nanofibers from a solution with 15 wt% P(MMA-co-AN) at different PPy contents: (a-b) 5.5 wt %; (c-d) 16 wt %; and (e-f) 24 wt %.

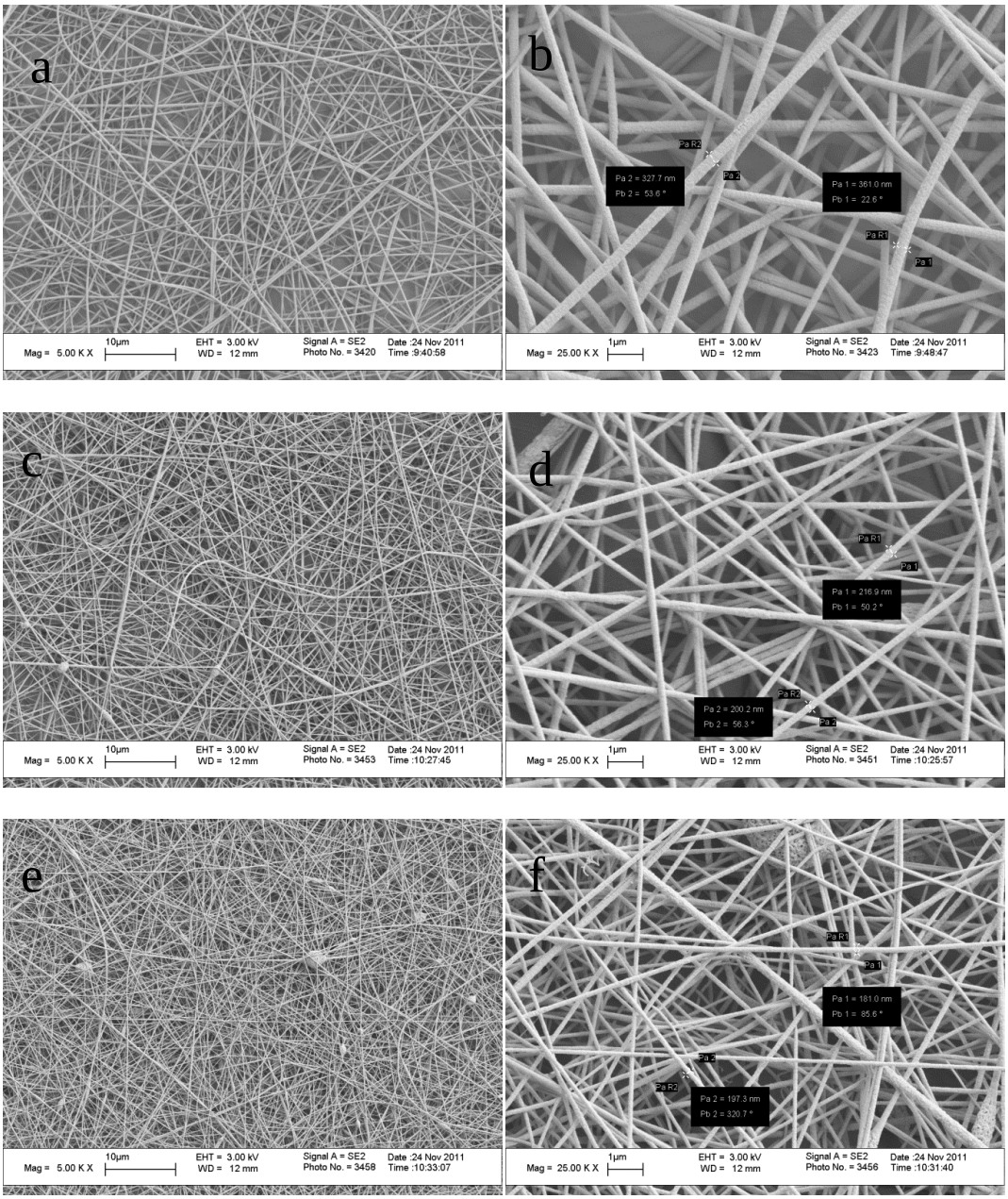

Figure 4.32 : Scanning electron micrographs of electrospun nanofibers from a solution with 15 wt% P(MMA-co-AN) at different PNPhPy contents: (a-b) 5.5 wt %; (c-d) 16 wt %; and (e-f) 24 wt %.

The morphologies of P(MMA-co-AN)/PNPhPy nanofibers are also characterized by SEM for 15 wt. % (Figure 4.32). According to SEM images, the diameter of P(MMA-co-AN)/PNPhPy nanofibers were reduced by initially added NPhPy concentration (Figure 4.33). With the increase of PNPhPy content, irregularities, such as so-called ‘beads on a string’ morphology, began to appear [88]. This may be a result of the increased conductivity and viscosity of the electrospinning solutions at higher PNPhPy contents [89].

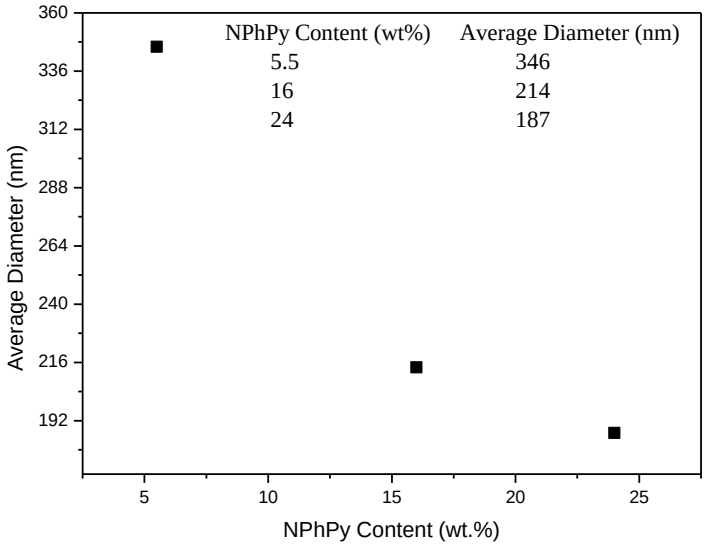

Figure 4.33 : Average nanofiber diameters of nanofibers electrospun from 15 wt% P(MMA-co-AN) solution at different NPhPy concentrations.

When the weight percentage of the initially added PNPhPy concentration varies from 5.5 % to 24 %, the average diameters of the nanofibers are reduced from 346 to 187 nm (Figure 4.33). The effect of fiber diameter on the electrical conductivity of PEDOT nanofibers indicated an increase in conductivity as the fiber diameter decreases from 260 nm to 140 nm. This could be attributed to the intrinsic fiber conductivity effect or the geometric surface and packing density or both, as a result of the reduction in fiber diameter [90]. The low average nanofiber diameters probably result from the relatively low molecular weight of conductive polymers [91]. Nanofibers have small average diameters when the solutions have higher conductivity [92]. The diameters of MWCNT-PAN nanofibers are decreased by increasing MWCNT concentrations. This reduction in diameters originates from the enhanced conductivity of the polymer solution with additional MWCNTs. It allows a large electric current during electrospinning and induces a large charge accumulation in the solution jet, resulting in strong electrostatic repulsion among the sprays. This repulsive force easily overcomes the surface tension of the jet to reduce diameters of the nanofibers [93].

Therefore, conducting polymer may act as a MWCNT and hence, the diameters of PNPhPy/P(MMA-co-AN) based nanofibers are decreased by increasing PNPhPy concentration. The nanofiber distribution in a unit area is increased by the addition of 24 wt% NPhPy (compared to 5.5 wt% NPhPy) (Figure 4.32).

5. CONCLUSION

Conducting polymer composites of PPy/P(MMA-co-AN), PNMPy/P(MMA-co-AN) and PNPhPy/P(MMA-co-AN) were synthesized by the oxidative matrix polymerization of pyrrole by Ce (IV) in the presence of P(MMA-co-AN). The formation and incorporation of PPy derivatives in the copolymer matrix were confirmed by FTIR-ATR and UV-Visible spectrophotmetric measurements. FTIR-ATR analysis of composite films supported the idea of cerium salt with nitrate ion act as a dopant. The increase in the a.c. electrical conductivity of the PPy derivatives/P(MMA-co-AN) composites over pure P(MMA-co-AN) was observed, also a linear increasing relationship was obtained between absorbance values of CH plane vibration of PPy derivatives (initially added Py derivatives) and conductivity values. At lower frequency up to 10^5 Hz, conductivity is independent of frequency; and at high frequencies between 10^5-10^7 Hz, conductivity is dependent of frequency due to polaron and bipolaron form of PPy derivatives which is only active at high frequency region. The dispersion of PPy derivatives particles in copolymer matrix was proven by SEM. In conclusion, composite thin films having PPy derivatives successfully introduced in P(MMA-co-AN) matrix which can be used for EMI shielding and absorbent panels. The mole fraction of AN in the P(MMA-co-AN) copolymer was determined to be 0.65 from the ^{1}H NMR spectrum. According to NMR analysis of PNPhPy/P(MMA-co-AN) and PPy/P(MMA-co-AN) composite thin films PNPhPy had broader more visible peaks with higher integral value at 7.0-8.5 ppm.

PPy derivatives/P(MMA-co-AN) multi-fuctional nanofibers were obtained from a well dispersed reaction medium by applying electrospinning method. The presence of PPy derivatives into nanofiber were represented by spectrophotometric and thermal measurements. SEM images indicated that the diameters of PPy derivatives/P(MMA-co-AN) nanofibers were dependent on initially added Py derivatives concentration. The polymerization of Py derivatives might induce a large electric current during electrospinning and allow a large charge accumulation in the

solution jet, therefore strong electrostatic repulsion among the sprays occurs. Thus, this repulsive force easily overcomes the surface tension of the jet to reduce diameters of the nanofibers.

REFERENCES

[1] **Aldissi, M., Poddar, P., Ram, M. K., Srikanth, H., and Yavuz, Ö.,** 2005: Polypyrrole composites for shielding applications, *Synthetic Metals*, **151**, 211-217.

[2] **Lin-Xia, W., Xin-Gui, L., Yu-Liang, Y.,** 2000: Preparation, properties and applications of polypyrroles, *Reactive & Functional Polymers*, **47**, 125-139.

[3] **Jang, J., Hak Oh, J.,** 2005: Fabrication of a Highly Transparent Conductive Thin Film from Polypyrrole/Poly(methyl methacrylate) Core/Shell Nanospheres, *Adv. Funct. Mater.*, **15**, DOI: 10.1002/adfm.200400095.

[4] **Dongkı, S., Doo, H. B., Jaechoon, C., Yongkeun, S., Youngkwan, L., and Yun, H. P.,** 1998: Ionic interactions in polyacrylonitrile/polypyrrole conducting polymer composite, *Journal of Applied Polymer Science*, **69**, 2641-2648.

[5] **Maity, A., Biswas, M.,** 2006: Water-Dispersible Conducting Nanocomposites of Polymethylmethacrylate-SiO2 Modified by Polyaniline and Polypyrrole, *J. Ind. Eng. Chem*, **12**, 626-634.

[6] **Lee, Y., Shin, D., Cho, J., Park, Y.H., Son, Y., Baik, D.H.,** 1998: Ionic Interactions in Polyacrylonitrile/Polypyrrole Conducting Polymer Composite. *Journal of Applied Polymer Science.*, **69**, 2641-2648.

[7**] Omastova, M., Simon, F.,** 2000: Surface characterizations of conductive poly(methyl methacrylate)/polypyrrole composites, *Journal of Materials Science*, **35,** 1743 – 1749.

[8] **Omastova, M., Micusik, M.,** 2012: Polypyrrole coating of inorganic and organic materials by chemical oxidative polymerisation, *Chemical Papers*, **66**, 392-414.

[9] **Dutta, P., De, S.K.,** 2003: Electrical properties of polypyrrole doped with β-naphthalenesulfonicacid and polypyrrole–polymethyl methacrylate blends, *Synthetic Metals*, **139**, 201-206.

[10] **Lee, C.Y., Lee, D.E., Joo, J., Kim, M.S., Lee, J.Y., Jeong, S.H., Byun, S.W.,** 2001: Conductivity and EMI Shielding Efficiency of Polypyrrole and Metal Compounds Coated on(non) Woven Fabrics, *Synthetic Metals*, **119**, 429-430.

[11] **Kuhn, H.H., Child, A.D., Kimbrell, W.C.,** 2000: Toward Real Applications of Conductive Polymers, *Synthetic Metals*, **71**, 2139-2142.

[12] **Bakhshi, A.K., Bhalla, G.,** 2004: Electrically conducting polymers: Materials of the twenty first century, *Journal of Scientific and Industrial Research*, **63**, 715-728.

[13] **Chiang, C.K., Fincher, C.R., Park, Y.W., Heeger, A.J., Shirakawa, H., Louis, F.J., Gau, S.C., MacDiarmid, A.G.** , 1977: *Phys. Rev. Lett.*, **39**, 578-580.

[14] **Chianella, I., Karras, K., Lakshmi, D., Whitcombe, M.J., Marson, S.,** 2012: Conductive Polymers for Plastic Electronics, *Molecularly Imprinted Sensors*, DOI: 10.1016/B978-0-444-56331-6.00012-8.

[15] **Margolis, J.,** 1989: Conductive Polymers and Plastics, *Chapman and Hall*, 121.

[16] **Margolis, J.,** 1989: Conductive Polymers and Plastics, *Chapman and Hall*, 120.

[17] **Barlow, A.,** 1997: Entone-OMI representative.

[18] **Alcacer, L.,** 1987: Conducting Polymers Special Applications , *D. Reidel Publishing Company*, 5.

[19] **Salaneck, W. R., Clark, D. T., Samuelsen, E. J.,** 1991: Science and Application of Conducting Polymers, *IOP Publishing*, 52, 55, 135, 168.

[20] **Alcacer, L.,** 1987: Conducting Polymers Special Applications, *D. Reidel Publishing Company*, 5, 192.

[21] **Bloor, D., Movagher, B.,** 1983, *IEEE proceedings***, 130,** 225**.**

[22] **Naarman, H., Theophilou, N.,** 1987, *Synth. Met.,***22**, 1.

[23] **Österholm, J.E. and co-workers,**1989, *Synth. Met.,***28**, 435-467.

[24] **Edwards, J. H., Feast, W. J., Bott, D. C.,** 1984, *Polymer*, **25**, 395.

[25] **Peter, J. S., Kaiser, F., Kaiser, A.B.,** 2004: Conducting Polymers, *Kirk-Othmer Encyclopedia of ChemicalTechnology*, DOI: 10.1002/0471238961.0512050318052514.a01.pub2

[26**] Percino, M.J., Chapela, V.M.,** 2013: Handbook of Polymer Synthesis, Characterization,and Processing, DOI: 10.1002/9781118480793.ch29.

[27] **Mort, N. F., Davis, E. A.,** 1979, *Electronic Processes in Non-Crystalline Materials*, Clarendon Press, Oxford.

[28] **Hapert, J. J.,** 2002: Hopping Conduction and Chemical Structure: a study on Silicon Suboxides,- Tekst., - Proefschrift Universiteit Utrecht 81.

[29] **Lubin, G.,** 1982, Handbook of Composites, *Van Nostrand Reinhold Company Inc.*, USA, 1,2.

[30]**Schwartz, M.M.,** 1997, Composite Materials, Volume I: Properties, Nondestructive Testing and Repair, *Prentice-Hall Inc.*, New Jersey, 10,11.

[31] **Sanjay, Mazumdar, K.,** 2002: Composites Manufacturing Materials, Product and Process Engineering, *CRC Press LLC*, USA, 4-6.

[32] **Cammarata, R.C.,** 2004: Nanocompopsites, *Introduction to Nanoscale Science and Technology*, 199-213, DOI: 10.1007/1-4020-7757-2_9.

[33] **Li, X. G., Yang, Y. L., and Wang, L. X.,** 2001: Preparation, Properties and Applications of Polypyrroles, *Reactive & Functional Polymers*, **47**, 125-139.

[34] **Pionteck, J., Omastova, M., Potschke, P., Simon, F., Chodak, I.,** 1999: Morphology, conductivity, and mechanical properties of polypyrrole-containing composites, *Journal of Macromolecular Science*, Part B, 38:5, 737-748.

[35] **Wallace, G.G., Spinks, G.M., Kane-Maguire, L.A.P., Teasdale, P.R.,** 2003: Conductive Electroactive Polymers, *Intelligent Materials Systems*, 2nd edition, CRC Press LCC, USA, 51.

[36] **Ansari, R.,** 2006: Polypyrrole conducting electroactive polymers: Synthesis and stability studies, *E Journal of Chemistry*, **3**, 186-201.

[37] **Erokhin, V., Ram, M. K., and Yavuz, Ö.,** 2008: *The New Frontiers of Organic and Composite Nanotechnology*. Elsevier Publishing, Oxford, England.

[38] **Omastova, M., Kosina, S., Pionteck, J., Janke, A., Pavlinec, J.,** 1996: Electrical properties and stability of polypyrrole containing conducting polymer composites, *Synthetic Metals*, **81**, 49-57.

[39] **Bai, H., Zhao, L., Lu, C., Li, C., Shia, G.,** 2009: Composite nanofibers of conducting polymers and hydrophobic insulating polymers: Preparation and sensing applications, *Polymer*, **50**, 3292–3301.

[40] **Han, G., Gaoquan Shi, G.,** 2007: Porous polypyrrole/polymethylmethacrylate composite film prepared by vapor deposition polymerization of pyrrole and its application for ammonia detection, *Thin Solid Films*, **515**, 6986-6991.

[41] **Nikpour, M., Chaouk, H., Mau, A., Chung, D., C., Wallace, G.,** 1998: Porous conducting membranes based on polypyrrole–PMMA composites, *Synthetic Metals*, **99**, 121–126.

[42] **Barde, W.S. , Pakade, S.V., Yawale, S.P.,** 2007: Ionic conductivity in polypyrrole-poly (vinyl acetate) films synthesized by chemical oxidative polymerization method, *Journal of Non-Crystalline Solids*, **353**, 1460-1465.

[43] **Çetiner, S., Ciobanu, R., Kalaoğlu, F., Karakaş, H., Kaya, N. U., Olariu, M., Saraç, A. S., and Ünsal, C.,** 2010: Polymerization of Pyrrole Derivatives on Polyacrylonitrile Matrix, FTIR-ATR and Dielectric Spectroscopic Chracterization of Composite Thin Film, *Synthetic Metals*, **160**, 1189-1196.

[44] **Herman, F., M.,** 2013: Encyclopedia of Polymer Science and Technology, *John Wiley & Sons*, 3rd edition, 34-36.

[45] **Liao, Y., Raoa, M., Li, W., Tana, C., Yia, J., Chena, L.,** 2009: Improvement in ionic conductivity of self-supported P(MMA-AN-VAc) gel electrolyte by fumed silica for lithium ion batteries, *Electrochimica Acta*, **54**, 6396–6402.

[46] **El-Aassar, M.R.,** 2012: Functionalized electrospun nanofibers from poly (AN-co-MMA) for enzyme immobilization, *Journal of Molecular Catalysis B: Enzymatic*, **85– 86**, 140–148.

[47] **Ambika-Prasad, M. V. N., and Murugendrappa, M. V.,** 2006: Dielectric Spectroscopy of Polypyrrole-Fe2O3 Composites, *Materials Research Bulletin*, **41**, 1364-1369.

[48] **Kao, K. C.,** 2004: *Dielectric Phenomena in Solids.* Elsevier Academic Press, Oxford, England.

[49] **Harun, M. H., Hussain, M. Y., Kassim, A., Mahmud, E., Mustafa, I. S., and Saion, E.,** 2009: Dielectric Properties of Poly(Vinyl Alcohol)/Polypyrrole Composite Polymer Films, *Journal for the Advancement of Science & Arts*, **1**, 9-16.

[50] **Andrade, C. A. D., de Melo, C. P., and de Oliveira, H, P.,** 2005: Optical and Dielectric Properties of Polypyrrole Nanoparticles in a Polyvinylalcahol Matrix, *Synthetic Metals*, **155**, 631-634.

[51] **Ambika-Prasad, M. V. N., Khasım, S., and Murugendrappa, M. V.,** 2005: Synthesis, Chracterization and Conductivity Studies of Polypyrrole-Fly Ash Composites, *Bulletin of Material Science*, **28**, 565-569.

[52] **Url-1** <*http://www.epa.gov* accessed at 10.04.2010.

[53] **Pethrick, R. A., Pielichowski, J., and Zaikov, G.E.,** 2004: *Monomers, Oligomers, Polymers, Composites and Nanocomposites Research: Synthesis, Properties and Applications.* Nova Science Publisher, New York, USA.

[54] **Url-2** <*http://www.ckpmac7.yz.yamatag-u.ac.jp*accessed at 10.04.2010.

[55] **Raoa, M.M., Liub, J.S., Li, W.S., Lianga, Y., Zhoua, D.Y.,** 2008: Preparation and performance analysis of PE-supported P(AN-*co*-MMA) gel polymer electrolyte for lithium ion battery application, *Journal of Membrane Science*, **322**, 314–319.

[56] **Zhoua, D.Y., Wanga, G.Z., Li, W.S., Li, G.L., Tana, C.L., Raoa, M.M., Liaoa Y.H.,** 2008: Preparation and performances of porous polyacrylonitrile–methyl methacrylate membrane for lithium-ion batteries, *Journal of Power Sources*, **184**, 477–480.

[57] **Liaoa, Y.H., Zhoua, D.Y., Raoa, M.M., Li, W.S., Caia, Z.P., Lianga, Y., Tana, C.L.,** 2009: Self-supported poly(methyl methacrylate–acrylonitrile–vinyl acetate)-based gel electrolyte for lithium ion battery, *Journal of Power Sources*, **189**, 139–144.

[58] **Tian, Z., He, X., Pu, W., Wan, C., Jiang, C,** 2006: Preparation of poly(acrylonitrile–butyl acrylate) gel electrolyte for lithium-ion batteries, *Electrochimica Acta*, **52**, 688–693.

[59] **Lee, Y.G., Park, J.K., Moon, S.I.,** 2000: Interfacial characteristics between lithium electrode and plasticized polymer electrolytes based on poly(acrylonitrile-co-methyl methacrylate), *Electrochimica Acta*, **46**, 533–539.

[60] **Kima, D.W., Kima, Y.R, Park, J.K., Moon, S.I.,** 1998: Electrical properties of the plasticized polymer electrolytes based on acrylonitrile-methyl methacrylate copolymers, *Solid State Ionics,* **106**, 329–337.

[61] **Patra, N., Barone, A.C., Salerno, M.,** 2011: Solvent Effects on the Thermal and Mechanical Properties of Poly(methyl methacrylate) Casted from Concentrated Solutions, *Advances in Polymer Technology*, **30**, 12–20.

[62] **Trigo, C.E.L., Porto, A.O., De Lima, G.M.,** 2004: Characterization of CdS nanoparticles in solutions of P(TFE-co-PVDF-co-Prop)/N,N-dimethylformamide, *European Polymer Journal,* **40**, 2465–2469.

[63] **Jacob, M.M.E., Arof, A.K.,** 2000: FTIR studies of DMF plasticized polyvinyledene fluoride based polymer electrolytes, *Electrochimica Acta,* **45**, 1701–1706.

[64] **Xing, S., Zhao, G.,** 2007: One-step synthesis of polypyrrole–Ag nanofiber composites in dilute mixed CTAB/SDS aqueous solution, *Materials Letters,* **61**, 2040–2044.

[65] **Yee, L.M., Mahmud, H.N.M.E., Kassim, A., Yunus, W.M.M.,** 2007: Polypyrrole-polyethylene glycol conducting polymer composite films: Preparation and characterization, *Synthetic Metals,* **157**, 386–389.

[66] **Sezer, E., Ustamehmetoglu, B., Sarac, A.S.,** 1999: Chemical and electrochemical polymerisation of pyrrole in the presence of *N*-substituted carbazoles, *Synthetic Metals,* **107**, 7–17.

[67] **Abdel-Wahab, Z.H., Mashaly, M.M., Faheim, A.A.,** 2005: Synthesis and Characterization of Cobalt(II), Cerium(III), and Dioxouranium(VI) Complexes of 2,3-Dimethyl-1-phenyl- 4-salicylidene-3-pyrazolin-5-one Mixed Ligand Complexes, Pyrolytic Products, and Biological Activities, *Chem. Pap.*, **59**, 25-36.

[68] **Vishnuvardhan, T.K., Kulkarni, V.R., Basavaraja, C., Raghavendra, S.C.,** 2006: Synthesis, characterization and a.c. conductivity of polypyrrole/Y2O3 composites, *Bull. Mater. Sci*., **29**, 77–83.

[69] **Wanga, W., Yua, D., Tiana, F.,** 2008: Synthesis and characterization of a new polypyrrole based on *N*-vinyl pyrrole, *Synthetic Metals,* **158**, 717–721.

[70] **Reung-U-Rai, A., Prom-Jun, A., Prissanaroon-Ouajai, W., Ouajai, S.,** 2008: Synthesis of Highly Conductive Polypyrrole Nanoparticles via Microemulsion Polymerization, *Journal of Metals, Materials and Minerals,* **18**, 27-31.

[71] **Puanglek, N., Sittattrakul, A., Lerdwijitjarud W.,** 2010: Enhancement of Electrical Conductivity of Polypyrrole and Its Derivative, *Sci. J. UBU,* **1**, 35-42.

[72] **Rizzi, M., Trueba, M., Trasatti, S.P.,** 2011 : *Synthetic Metals*, **161**, 23–31.

[73] **Tarkuc, S., Sahin, E., Toppare, L., Colak, D., Cianga, I., Yagci, Y.,** 2006: Synthesis, characterization and electrochromic properties of a conducting copolymer of pyrrole functionalized polystyrene with pyrrole, *Polymer*, **47**, 2001–2009.

[74] **Habbeb, M.A., Hashim, A., AbidAli, A.R.K.,** 2011: The Dielectric Properties for (PMMA-LiF) Composites, *European Journal of Scientific Research*, **61**, 367-371.

[75] **Harun, M.H., Saion, E., Kassim, A., Mahmud, E., Hussain, M.Y., Mustafa, I.S.,** 2009: Dielectric Properties of Poly (vinyl alcohol)/Polypyrrole Composite Polymer Films, *Journal for the advancement of scıence & arts,***1**, 9-16.

[76] **Narula, A.K., Ramadhar, S., Subhas, C.,** 2000: Low frequency ac conduction and dielectric relaxation in poly(N-methyl pyrrole), *Bull. Mater. Sci.,* **23**, 227-232.

[77] **Hamciuc, C., Hamciuc E., Ipate, A.M., Okrasa, L.,** 2008: Copoly(1,3,4-oxadiazole-ether)s containing phthalide groups and thin films made therefrom, *Polymer*, **49**, 681-690.

[78] **Saafan, S.A., El-Nimr, M.K., El-Ghazzawy, E.H.,** 2006: Study of Dielectric Properties of Polypyrrole Prepared using Two Different Oxidizing Agents, *Journal of Applied Polymer Science,* **99**, 3370-3379.

[79] **Abdullah, O.G., Hussen, S.A., Alani, A.,** 2011: Electrical Characterization of Polyvinyl Alcohol Films Doped with Sodium Iodide, *Asian Transactions on Science & Technology*, **1**, 1-4.

[80] **Murugendrappa, M.V., Parveen, A., Ambika Prasad, M.V.N.,** 2007: Synthesis, characterization and ac conductivity studies of polypyrrole–vanadium pentaoxide composites, *Materials Science and Engineering A,* **459**, 371-374.

[81] **Han, G., Shi, G.,** 2007: Porous polypyrrole/polymethylmethacrylate composite film prepared by vapor deposition polymerization of pyrrole and its application for ammonia detection, *Thin Solid Films*, **515**, 6986-6991.

[82] **Shirale, D.J., Gade, V.K., Gaikwad, P.D., Savale, P.A., Shirsat, M.D.,** 2007: Galvanostatic deposition of Poly(N-methylpyrrole) film with various dopants and co-dopants: A comparative study, *Materials Letters,* **61**, 1372-1375.

[83] **Sarac, A.S., Sezgin, S., Ates, M., Turhan, C.M., Parlak, E.A., Irfanoglu, B.,** 2008: Electrochemical impedance spectroscopy of poly(*N*-methyl pyrrole) on carbon fiber microelectrodes and morphology, *Progress in Organic Coatings,* **62**, 331-335.

[84] **Wei, M., Lu, Y.,** 2009: Templating fabrication of polypyrrole nanorods/nanofibers, *Synthetic Metals,* **159**, 1061-1066.

[85] **Dallas, P., Niarchos, D., Vrbanic, D., Boukos, N., Pejounik, S., Trapalis, C., Petridis, D.,** 2007: Interfacial polymerization of pyrrole and in situ synthesis of polypyrrole/silver nanocomposites, *Polymer,* **48**, 2007-2013.

[86] **Huang, K., Wan, M., Long, Y., Chen, Z., Wei, Y.,** 2005: Multi-functional polypyrrole nanofibers via a functional dopant-introduced process, *Synthetic Metals,* **155**, 495-500.

[87] **Ak, M., Gacal, B., Kiskan, B., Yagci, Y., Toppare, L.,** 2008: Enhancing electrochromic properties of polypyrrole by silsesquioxane nanocages, *Polymer*, **49**, 2202-2210.

[88] **Chronakis, I. S., Grapenson, S., and Jakob, A.,** 2006: Conductive Polypyrrole Nanofibers via Electrospinning: Electrical and Morphological Properties, *Polymer*, **47**, 1597-1603.

[89] **El-Aufy, A., Nabet, B., and Ko, F.,** 2003: Carbon Nanotube Reinforced Nanocomposites for Wearable Electronics, *Polymer Preprint*, **44**, 134-135.

[90] **Andrady, A. L.,** 2008: *Science and Technology of Polymer Nanofibers*. John Wiley & Sons Inc., New Jersey, USA.

[91] **Ra, E. J., An, K. H., Kim, K. K., Jeong, S. Y., and Lee, Y. H.,** 2005: Anisotropic Electrical Conductivity of MWCNT/PAN Nanofiber Paper, *Chemical Physics Letters* , **413**, 188-193.

[92] **Andrady, A. L.,** 2008: *Science and Technology of Polymer Nanofibers*. John Wiley & Sons Inc., New Jersey, USA. 60.

[93] **Ra, E. J., An, K. H., Kim, K. K., Jeong, S. Y., and Lee, Y. H.,** 2005: Anisotropic Electrical Conductivity of MWCNT/PAN Nanofiber Paper, *Chemical Physics Letters* , **413**, 188-193.

CURRICULUM VITAE

Name Surname: Ulviye DALGIÇ

Place and Date of Birth: Kırcaali/BULGARİSTAN, 02.03.1981

E-Mail: ulviye.dalgic@gmail.com

EDUCATION:

B.Sc.: Izmir Institute of Technology, Chemical Engineering (2002-2007)